Author's Response

First of all, we'd like to thank the referees and editors, the comments and advices they mentioned help us a lot to improve the manuscript. We modify the manuscript with more general description and some of our new insight.

Replys to Anonymous Referee #1

Thank you very much for reading our manuscript meticulously, those problems you found and the advices you mentioned, help us a lot to improve the description and strictness to the manuscript. There are some opinions we'd like to discuss and share with you.

The main theme of this manuscript is finding out a method to extend the square conservation scheme, from regular latitude-longitude grid to an arbitrarily structured C-grids dynamic core, TRiSK, meanwhile, the intrinsic property of TRiSK (including accuracy of operators and conservation properties) should not be broken down.

There are some problems with the presentation in the manuscript (details below), which it should be possible to fix. However, the key ideas needed to obtain exact energy conservation on arbitrary meshes have been around for a while; this paper merely brings them together. Also, temporal truncation errors tend to be much smaller than spatial truncation errors in atmospheric models, so only a small improvement (if any) is obtained by replacing an energy-conserving spatial discretization by an energy-conserving space-time discretization, (as the results in this paper confirm). Thus, I think the manuscript lacks the originality and significance needed to justify publication in GMD.

Reply:

The most of so-called energy conservation schemes on arbitrary meshes merely conserve total energy within time truncation error, i.e. (Ringler et al,2010), (Thi-Thao-Phuong Hoang,2019), the energy is still slightly dissipative during temporal integration. As Eq.(24) in the manuscript, the energy is strictly conserved only if $2\tau_n(\varphi^n, F^n) + {\tau_n}^2\|\varphi^n\|^2 = 0$, unfortunately, most of temporal integration schemes do not satisfy this condition. Conserving energy within time truncation error is not equivalent to strict/exact energy conservation, the former allows slightly energy dissipative/anti-dissipative during temporal integration, the later conserving total energy in round-off error. In the manuscript, Figure 3c, Figure 4c and Figure 5c (the same as the following figures, from left to right) are showing the differences between "Conserving energy within truncation error" (blue line) and "Strictly conserving energy" (red line).

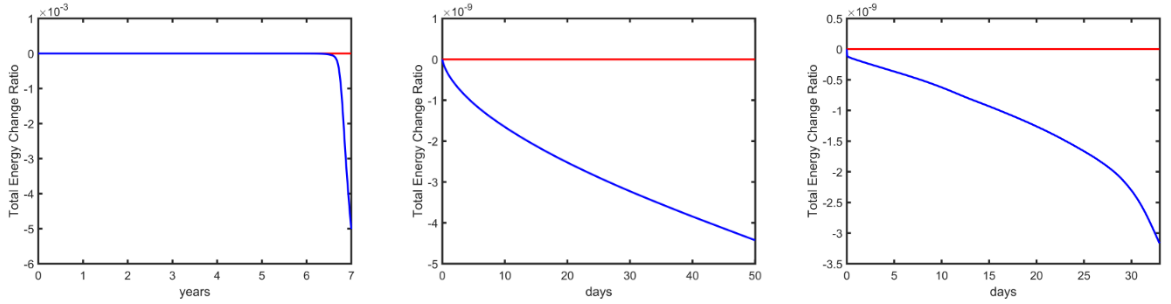

Indeed, there are some methods to exactly conserve energy on arbitrary meshes, i.e. taking energy as an evolution variable, based on conservation law, the energy flux is balanced between each cell, therefore energy is conserved anywhere and anytime (Satoh, 2004, Section 1.2.3). But these methods are not quadratic conservation in mathematics. In the shallow water system, one can obtain the exact energy conservation by replacing the continuous equation by energy equation, but this method sacrifices mass conservation; or in another way, replacing the momentum equation by energy equation, but the flow direction will not able to be determined, and sometimes worse situation appears, since the lack of constrain from momentum equation, potential energy could be greater than total energy, which result in the wind speed becomes imaginary number.

By implementing the square conservation scheme, neither momentum equation nor continuous equation needs to be replaced by energy equation, the total energy is strictly conserved, rather than conserved within time truncation error, meanwhile, there are not influences to the other conservative properties, such as mass and absolute vorticity.

About the originality. The prerequisite of implementing square conservation scheme is that the spatial discrete operator must be anti-symmetrical, but it is hard to construct an anti-symmetrical operator on quasi-uniform grids directly, therefore we try to find another way to obtain the anti-symmetrical operator. Energy conservation is one of the intrinsic properties of TRiSK shallow water dynamic core, and as we mentioned in Section 3.2, Eq.(13) is the key to connecting square conservation and energy conservation, by using this simple combination of original TRiSK spatial discrete operators, the anti-symmetrical operator is built.

Note that, for constructing the anti-symmetrical operator in shallow water system, the units of the evolution variables must be unified, otherwise, the addition is not able to operate between different variables, this is the reason we take IAP transformation. Improving the conservation property is not like improving accuracy of the model, the convergence rate of spatial discrete operator, and the accuracy of temporal integration scheme are not changed in our study. Indeed, the reductions of errors are not such significant, but the physical characteristics are more analogous to the real system. The differences are not obvious in short term simulation, but in long term simulation, the advantage of strict energy conservation scheme may be huge, this is intuitively showed by the numerical test in (Wang,1996), which we'd like to share with you in Response for specific comment #2.

In the following content, we response your specific comments.

Response for specific comment #1:

Sections 3.1, 3.2. The notation $\mathcal{L}F$, $\mathcal{M}u$, $\mathcal{N}\phi$ suggests that $\mathcal{L}$, $\mathcal{M}$, $\mathcal{N}$ are linear functions of F, u, and - respectively. In fact they are all nonlinear functions. Moreover, $\mathcal{M}$ and $\mathcal{N}$ are actually functions of both u and ϕ. These two sections are over-elaborate and presented in a very confusing way. In several places it is not obvious what is assumed and what is claimed to be proved. All that is really needed is the fact that the energy at a point can be written as a squared quantity by making a certain change of variables.

Reply:

Thank you for reminding, indeed, the derivation does not depend on the linear operation, but indeed the expression is not strict enough. The following expression is better

$$\begin{cases} \frac{\partial \boldsymbol{u}}{\partial t} + \mathcal{M}(\phi, u) = 0 \\ \frac{\partial \phi}{\partial t} + \mathcal{N}(\phi, u) = 0 \end{cases},$$

For simplify expression, we write $\mathcal{M} = \mathcal{M}(\phi, u), \mathcal{N} = \mathcal{N}(\phi, u)$

$$\frac{\partial \boldsymbol{U}}{\partial t} = \sqrt{\phi}\frac{\partial \boldsymbol{u}}{\partial t} + \frac{\boldsymbol{u}}{2\sqrt{\phi}}\frac{\partial \phi}{\partial t} = -\sqrt{\phi}\mathcal{M} - \frac{\boldsymbol{u}}{2\sqrt{\phi}}\mathcal{N}$$

$$(\mathcal{L}(\boldsymbol{F}), \boldsymbol{F}) = -\left(\frac{\partial \boldsymbol{U}}{\partial t}, \boldsymbol{U}\right) - \left(\frac{\partial \phi}{\partial t}, \phi\right)$$

$$= \oiint_{\Omega} -\boldsymbol{U}\frac{\partial \boldsymbol{U}}{\partial t} - \phi\frac{\partial \phi}{\partial t}\, ds$$

$$= \oiint_{\Omega} -\boldsymbol{U}\left(-\sqrt{\phi}\mathcal{M} - \frac{\boldsymbol{u}}{2\sqrt{\phi}}\mathcal{N}\right) + \phi\mathcal{N}\, ds$$

$$= \oiint_{\Omega} \phi u \cdot \mathcal{M} + \frac{|\boldsymbol{u}|^2}{2}\mathcal{N} + \phi\mathcal{N}\, ds$$

$$= (\mathcal{M}, \phi u) + (\mathcal{N}, E)$$

$$= 0$$

All of the similar expressions are fixed in the new version manuscript.

About "the energy at a point can be written as a squared quantity by making a certain change of variables", this is what we are talking about in Section 3.1, the square conservation is equivalent to energy conservation in a continuous system.

Response for specific comment #2:

P1 line 27, also P2 lines 3-5. The opening sentence is too categorical. For a quantity like energy or potential enstrophy, in a numerical model the total is made up of resolved and unresolved contributions. Therefore, it is not obvious that conserving the resolved contribution is necessary for a good solution; indeed, it may be necessary to dissipate the resolved contribution (e.g. to prevent 'spectral blocking'). One can argue for a conservative numerical method by saying that we want to parameterize any dissipation, not leave it to numerical errors, but the opposite argument can also be made. Such ideas are extensively discussed in the literature.

Reply:

Indeed, there are resolvable and unresolvable energy contributions. Since the model resolution is not able to reach a molecule level, the numerical model cannot resolve all the mass, there are resolvable and unresolvable mass contributions either, as widely known, it's hard to obtain a good result without total mass conservation. For total energy, the influence is not significant in short-term simulation, but the long-term simulation, without total energy conservation, often lead to a terrible result.

On the other hand, energy conservation is one of the intrinsic conservation properties of the spatial discrete operator in TRiSK shallow water dynamic core (Ringler et al, 2010, Section 3.7), however, this property is lost during temporal integration by using original Runge-Kutta scheme. The temporal integration scheme brings time truncation error into the model, rather than spatial discrete operator, which means that the temporal integration scheme makes the model loses one of the intrinsic properties which is provided by spatial discrete scheme.

Figure 3c in the manuscript, a detail is that the square conservation scheme strictly conserves energy, even though the steady geostrophic flow collapses, but the original TRiSK scheme cannot maintain the total energy after collapse, this is an obvious difference between the "Conserving energy within truncation error" and "Strictly conserving energy". The reason is that the square conservation scheme maintains the conservation properties of spatial discrete operators faithfully, but original temporal integration scheme does not.

An interesting example can be found in (Wang, 1996), the numerical test of the linear ODE

$$\begin{cases} \dfrac{dx}{dt} = -ay \\ \dfrac{dy}{dt} = bx \end{cases}$$

the true solution of the equation is an ellipse conform to $bx^2 + ay^2 = c$ (c is a constant), after long term numerical simulation (after 10^8 steps) with original Runge-Kutta, the generalized energy tends to zero, and the solution tends to a single point (Fig. 2(a), Wang, 1996, as showing as follow), but the Runge-Kutta with square conservative property is able to maintain the generalized energy strictly conserved, and the solution is still a ellipse as initial time (Fig. 2(b) , Wang, 1996).

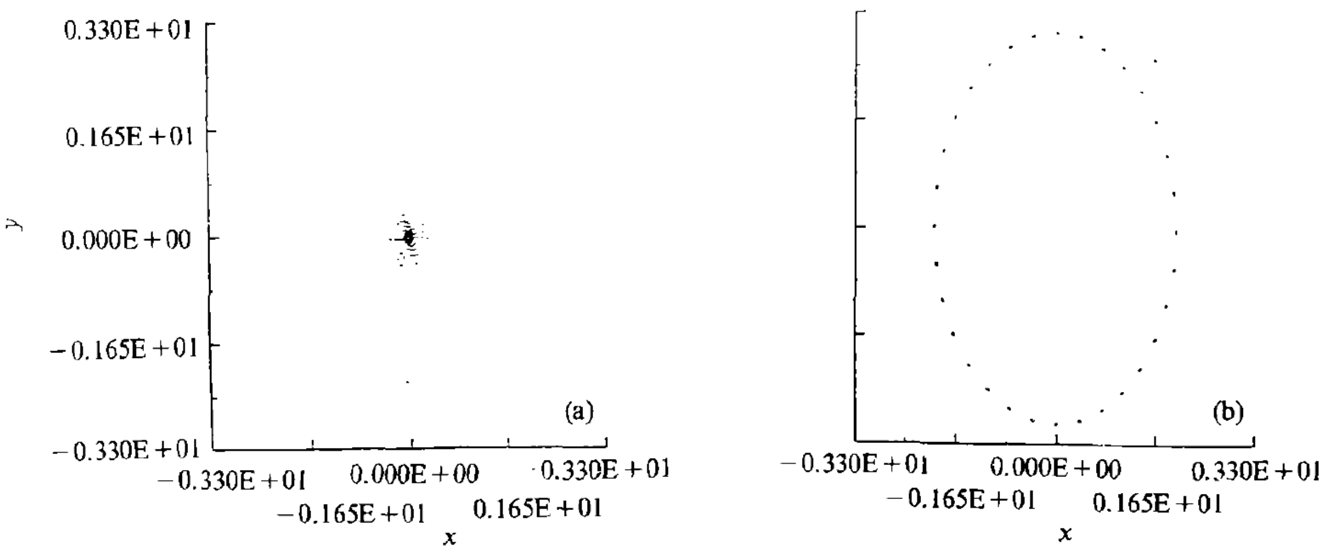

Fig. 2. Results from the 10^8-step integration (printing a result per 10^5 steps). (a) By the old Runge-Kutta scheme, (b) by the new Runge-Kutta scheme.

This class of Runge-Kutta scheme with square conservative property is exactly what we mentioned in the manuscript Section 3.3.

Response for specific comment #3:

P1 line 29, Figs. 3b, 5b, 7b, P19 line 17. On a spherical domain the vanishing of the global integral of vorticity is a purely kinematic identity. Provided the vorticity and its integral are calculated in a self-consistent way, the same result must hold in the discrete case (e.g. P10 line 20). Thus, conservation of the global integral of vorticity is a test only of the fact that the vorticity is calculated consistently; it says nothing about the properties of the numerical methods used to solve the equations.

Reply:

Total absolute vorticity conservation is one of the intrinsic properties of TRiSK shallow water dynamic core, in the manuscript, we are not trying to discuss the importance of absolute vorticity conservation, but to maintain the total energy conservation without breaking down the intrinsic properties of TRiSK, The figures and the demonstrations about the conservation of total absolute vorticity are here to prove that the square conservation scheme has no influence to the other conservation properties of TRiSK shallow water dynamic core.

Response for specific comment #4:

P1 line 29. '...five basic physical conserved properties'. Actually potential enstrophy is just one member of an infinite family (so-called Casimirs).

Reply:

Thank you for reminding, indeed, potential enstrophy is one member of an infinite family, in the manuscript, we are not tending to discuss all of the invariants, the description about five basic physical conservative properties is based on (Wang, 2008).

Response for specific comment #5:

P3 line 23. This form of the equations is usually called ‘vector-invariant’ (as on P19 line 16).

Reply:

Indeed, thank you very much, it has been fixed in the new version of manuscript

Response for specific comment #6:

P4. Equation (3) is inconsistent with the definition of the 2-norm on line 5. This paragraph seems to be mixing up point values and global integrals.

Reply:

Indeed, the total energy should be defined as follow

$$\oiint_{\Omega} \epsilon \, ds = \oiint_{\Omega} g\epsilon_{R10} \, ds = \oiint_{\Omega} \phi K + \frac{1}{2}\phi^2 + \phi\phi_s \, ds = \|\phi K\| + \left\|\frac{1}{2}\phi^2\right\| + \|\phi\phi_s\|$$

Response for specific comment #7:

Figure 1. Note that the grid used need not be uniform and regular (as suggested by the figure).

Reply:

Indeed, uniform and non-uniform grid do not influence the location of the variables and the structure of spatial discrete operators are the same as well. The square conservation scheme is available on arbitrarily structured C-grids as the title of the manuscript. As shown in Fig.1, Fig.2, Fig.3, (Ringler et. al, 2010), the regular is clear to introduce the structure of the SCVT mesh.

Response for specific comment #8:

P5. Note that the sign convection for u_e is related to the direction of the unit normal -this is crucial to get everything to work out. Also crucial for energy conservation is that $Q_e^{\perp}$ is constructed to satisfy the equation on P20 line 9.

Reply:

The description of indicator function $n_{e,i}$ for identifying the direction of u_e can be found in the end of Section 2, $n_{e,i}$ appears in all of the correlative derivations in the manuscript.

The spatial discrete operators, that we described in the manuscript, are the same as those in (Ringler et al., 2010), we construct the anti-symmetrical spatial discrete operator by using the original spatial discrete operator in TRiSK shallow water dynamic core, therefore, all of the properties, mentioned by (Ringler et. al,2010), are still applicable in the manuscript. Indeed, there are two methods of calculating $Q_e^{\perp}$ in (Ringler et al,2010), in our manuscript, the algorithm of calculating $Q_e^{\perp}$ satisfies the condition to keep energy conservation, which is described in Section 3.7.2, Ringler et al. (2010).

Response for specific comment #9:

P5 line 22. '...new type of Runge-Kutta'. Not so new (1996).

Reply:

It is not so new, we try not to modify the title of (Wang, 1996), "A Class of New Explicit Runge-Kutta Schemes", in the new version of manuscript, this expression is changed.

Response for specific comment #10:

P6 line 11. It would be helpful to give a reference for 'IAP transformation'.

Reply:

The earliest description about IAP transformation can be found in (Section 2, Zeng, 1987), and also cited by (Wang, 2004).

Response for specific comment #11:

P11 lines 22-23. The text does not make sense - it seems to be mixing up point values and global integrals.

Reply:

Indeed, there is a mistake, the error measure function should be $I(X^n) = \frac{S(X_i^n) - S(X_i^0)}{S(X_i^0)}$, where $S(X) = \frac{\sum_{i=1}^{N} X(i)A(i)}{\sum_{i=1}^{N} A(i)}$, X_i^n is the variable at the nth time point on the ith cell and X_i^0 is the variable at the initial time, and $A(i)$ is the area of the ith cell. This is similar to (135)-(140), Williamson, 1992, but the coordinate is no longer latitude-longitude, in the quasi-uniformed grid, the weight is now area of each cell. For a simpler expression $I(X^n) = \frac{\sum_{i=1}^{N} (X_i^n - X_i^0) A(i)}{\sum_{i=1}^{N} X_i^0 A(i)}$, the result is equivalent to the former expression.

Response for specific comment #12:

Section 5.2. The fact that the solid body rotation flow eventually breaks down, despite the conservation properties of the scheme, is intriguing. Could this be a manifestation of the 'Hollingsworth instability' (as discussed, for example, in Skamarock et al 2012)?

Reply:

We are not sure the connection between the collapse of steady geostrophic flow and 'Hollingsworth instability', but we found another way to delay the collapse, we observed that once we site the cell centers on two poles, the poles are just like the sources of errors, so we tried to rotate the mesh, and did not let any cell center site on poles, the errors was much more smaller, and the collapse has delayed obviously. Therefore, in our opinion, the principal cause of collapse is not the conservation properties, but maybe something like polar singularity, as we mentioned in the manuscript, maintaining the strict energy conservation just delays the collapse, this phenomenon needs further study.

Response for specific comment #13:

P19 line 26. Sign error? Line 30. What is h_e?

Reply:

Thanks a lot.

P19 line 26 should be $\left(U,\frac{\partial U}{\partial t}\right)_e+\left(\phi,\frac{\partial \phi}{\partial t}\right)_i=0$, and line 30 should be $\left(U,\frac{\partial U}{\partial t}\right)_e=\sum_{e=1}^{nEdges}U_e\left(C_e\frac{\partial u_e}{\partial \mathrm{t}}+\frac{u_e}{2C_e}\frac{\partial \phi_e}{\partial \mathrm{t}}\right)A_e$

Even though, there is no influence to the result, these errors shouldn't be happened.

Response for specific comment #14:

References are not in alphabetical order.

Reply:

This problem is fixed in new version of manuscript. Thank you for reminding.

Replys to Anonymous Referee #2

We would like to thank you for the positive comments and constructive advices, which help us to make the manuscript more clearly and more persuasive. The responses for the comments are in following text.

Response for specific comment #1:

The necessity to conserve the resolved energy in numerical solutions to an energy conservation system is actually the same as that to conserve the resolved mass. To highlight the significance of constructing an energy conservation scheme for the TRiSK dynamic core, a clear explanation on the necessity should be provided in Section 1.

Reply:

This is a good advice, energy conservation is an important property for the closed physical system, the shallow water system without any energy sink or source is one of the closed system, and the numerical model such as TRiSK shallow water dynamic core is a kind of approximation to the closed system, therefore, the basic integral invariants should be conserved, as we cited from (Arakawa, 1977), the maintenance of integral make the physics of the discrete model more analogous to the physics of the continuous atmosphere, and on the other hand make the errors less systematic. Another interesting example could be found in (Wang, 1996), the numerical test of the linear ODE

$$\begin{cases} \frac{dx}{dt} = -ay \\ \frac{dy}{dt} = bx \end{cases}$$

the true solution of the equation is an ellipse conform to $bx^2 + ay^2 = c$ (c is a constant), but after long term numerical simulation (after 10^8 steps) with original Runge-Kutta, the generalized energy tends to zero, and the solution tends to a single point(Fig.2, Wang, 1996). I think it's clearly to see the importance of keeping energy conservation. The references are packed in the zip file.

Response for specific comment #2:

Line 19/Page 2: CRK is improperly used as the abbreviation of "a new class of Runger-Kutta scheme", because the word "class" does not describe the main characteristics of this scheme. NRK is better.

Reply:

CRK stands for Conservative Runge-Kutta in my opinion, which means this kind of Runge-Kutta helps make the square conservation, it's just an abbreviation, but of course, the naming right belongs to the proposer of the scheme, Bin Wang. I use this abbreviation just to make the article concise.

Response for specific comment #3:

I wonder why the title of Section 2 is exactly the same as that of Section 1 (Lin 22/Page 3).

Reply:

Thank you for finding out the problem. The right title of Section 2 is "Introduction of TRiSK".

Response for specific comment #4:

The equality (3) (Line 4/Page 4) is not true, which missed the integration sign after the second equal mark.

Reply:

Indeed, the total energy should be defined as follow

$$\oiint_{\Omega} \epsilon \, ds = \oiint_{\Omega} g\epsilon_{R10} \, ds = \oiint_{\Omega} \phi K + \frac{1}{2}\phi^2 + \phi\phi_s \, ds = \|\phi K\| + \left\|\frac{1}{2}\phi^2\right\| + \|\phi\phi_s\|$$

Response for specific comment #5:

The semi-discrete form of the shallow water equation set [Equations (4)-(5) on Lines 4-5/Page 5] should no longer be a partial differential equation set, but an ordinary differential equation set.

Reply:

We are trying to express the same discrete system as which in (Ringler, 2010) Eqs.(19)-(20), you're right, "semi-discrete form" should be modified to "discrete system".

Response for specific comment #6:

Line 6/Page 5: u and v are not the variables of Eqs.(4)-(5).

Reply:

You are right, u is the evolution variable for the equation, v does not appear in Eqs.(4) and (5).

Response for specific comment #7:

Line 20/Page 7: The equality is not true, because a negative sign is missed before (not sure, but there is only one equation)

Reply:

Indeed, the derivation should be

$$\begin{cases} \frac{\partial \boldsymbol{u}}{\partial t} + \mathcal{M}(\phi, u) = 0 \\ \frac{\partial \phi}{\partial t} + \mathcal{N}(\phi, u) = 0 \end{cases},$$

For simplify expression, we write $\mathcal{M} = \mathcal{M}(\phi, u), \mathcal{N} = \mathcal{N}(\phi, u)$

$$\frac{\partial \boldsymbol{U}}{\partial t} = \sqrt{\phi}\frac{\partial \boldsymbol{u}}{\partial t} + \frac{\boldsymbol{u}}{2\sqrt{\phi}}\frac{\partial \phi}{\partial t} = -\sqrt{\phi}\mathcal{M} - \frac{\boldsymbol{u}}{2\sqrt{\phi}}\mathcal{N}$$

$$(\mathcal{L}(\boldsymbol{F}), \boldsymbol{F}) = -\left(\frac{\partial \boldsymbol{U}}{\partial t}, \boldsymbol{U}\right) - \left(\frac{\partial \phi}{\partial t}, \phi\right)$$

$$= \oiint_{\Omega} -\boldsymbol{U}\frac{\partial \boldsymbol{U}}{\partial t} - \phi\frac{\partial \phi}{\partial t}\ ds$$

$$= \oiint_{\Omega} -\boldsymbol{U}\left(-\sqrt{\phi}\mathcal{M} - \frac{\boldsymbol{u}}{2\sqrt{\phi}}\mathcal{N}\right) + \phi\mathcal{N}\ ds$$

$$= \oiint_{\Omega} \phi u \cdot \mathcal{M} + \frac{|\boldsymbol{u}|^2}{2}\mathcal{N} + \phi\mathcal{N}\ ds$$

$$= (\mathcal{M}, \phi u) + (\mathcal{N}, E)$$

$$= 0$$

This problem does not influence the conclusion, thank you for checking the derivation meticulously.

Response for minor comment #8:

Line 10/Page 1: “The square conservation theory is widely used on latitude-longitude grids” –> “The square conservation law is maintained in the dynamic cores on latitude-longitude grids”.

Reply:

The square conservation scheme is implemented in The Grid-point Atmospheric Model of IAP LASG(GAMIL), and the result of GAMIL was published in CMILP5, but your advice is good.

Response for minor comment #9 and #10:

9) Line 4/Page 2: “which is” –> “which are”.

10) Line 26/Page 2: “polar problem” –> “polar instability” or “polar singularity”.

Reply:

Thank you for finding out those mistakes, they are fixed in the 4th version of manuscript.

List of relevant changes made in the manuscript

1. Switch all of the CRK to NRK.
2. In Abstract, we fix some description of square conservation and add more introductions of two kinds of energy conservation scheme.
3. In Introduction
   (1) Add more references to introduce the importance of energy conservation
   (2) Expound the differences between conserving energy in time truncation-error and conserving energy in round-off error.
   (3) Switch "polar problem" to "polar singularity".
4. In Section 2
   (1) Switch "flux format" to "vector-invariant format"
   (2) Fix the mistake of total energy expression as
   $$\oiint_{\Omega} \epsilon\, ds = \oiint_{\Omega} g\epsilon_{R10}\, ds = \oiint_{\Omega} \phi K + \frac{1}{2}\phi^2 + \phi\phi_s\, ds = \|\phi K\| + \left\|\frac{1}{2}\phi^2\right\| + \|\phi\phi_s\|$$
   (3) Add description for Figure 1.
   (4) Modify some other details.
5. In Section 3
   (1) Add references about IAP transformation.
   (2) Switch $\mathcal{L}F$ to $\mathcal{L}(F)$
   (3) Switch LF to $L(F)$
   (4) Switch operators $\mathcal{M}$ and $\mathcal{N}$ to function $\mathcal{M} = \mathcal{M}(\phi, u)$ and $\mathcal{N} = \mathcal{N}(\phi, u)$
   (5) Switch operators M and N to function $M = M(\phi, u)$ and $N = N(\phi, u)$
   (6) Add description of $\sqrt{\phi_e}$ and ϕ_e.
   (7) Correct the sign for Eq.(20)
   (8) Modify some other details.
6. In Section 5
   (1) Add description of the differences between conserving energy in time truncation-error and conserving energy in round-off error during entire temporal integration period.
   (2) Correct $I(X^n) = \frac{s(x_i^n) - s(x_i^0)}{s(x_i^n)}$ to $I(X^n) = \frac{s(x_i^n) - s(x_i^0)}{s(x_i^0)}$
   (3) Add the discussion about the benefits of implementing square conservation scheme in TRiSK in the end of this section.
7. In Appendix A
   (1) Correct $\left(U, \frac{\partial U}{\partial t}\right)_e = \left(\phi, \frac{\partial \phi}{\partial t}\right)_i$ to $\left(U, \frac{\partial U}{\partial t}\right)_e + \left(\phi, \frac{\partial \phi}{\partial t}\right)_i = 0$
   (2) Correct $\left(U, \frac{\partial U}{\partial t}\right)_e = \sum_{e=1}^{nEdges} U_e \left(C_e \frac{\partial u_e}{\partial \mathrm{t}} + \frac{u_e}{2h_e}\frac{\partial \phi_e}{\partial \mathrm{t}}\right) A_e$ to $\left(U, \frac{\partial U}{\partial t}\right)_e = \sum_{e=1}^{nEdges} U_e \left(C_e \frac{\partial u_e}{\partial \mathrm{t}} + \frac{u_e}{2C_e}\frac{\partial \phi_e}{\partial \mathrm{t}}\right) A_e$
8. In References, we adjust the sequence of the references to fit the alphabetical order.

Extending Square Conservation to Arbitrarily Structured C-grids with Shallow Water Equations

Lilong Zhou[1,3], Jinming Feng[2], Lijuan Hua[1]

[1]College of Earth and Planetary Sciences, University of Chinese Academy of Sciences
[2]Key Laboratory of Regional Climate-Environment for Temperate East Asia, Institute of Atmospheric Physics, Chinese Academy of Sciences
[3]Numerical Weather Prediction Center of China Meteorological Administration

Correspondence to: Jinming Feng (fengjm@tea.ac.cn)

Abstract. The square conservation law is implemented in the atmospheric dynamic cores on latitude-longitude grids~~The square conservation theory is widely used on latitude–longitude grids~~, but it is rarely implemented on quasi-uniform grids, given the difficulty involved in constructing anti-symmetrical spatial discrete operators on these grids. Increasingly more models are developed on quasi-uniform grids, such as arbitrarily structured C-grids. Thuburn–Ringler–Skamarock–Klemp (TRiSK) is a shallow water dynamic core on an arbitrarily structured C-grid. The spatial discrete operator of TRiSK is able to naturally maintain the conservation properties of total mass, total absolute vorticity and ~~instantaneous~~conserving total energy with time truncation error~~. T~~, the first 2 integral invariants are ~~entirely~~ exactly conserved during integration, but the total energy dissipates when using the dissipative temporal integration schemes, i.e., Runge-Kutta. The method of strictly conserving the total energy simultaneously, which means conserving energy in round-off error during entire temporal integration period, uses both an anti-symmetrical spatial discrete operator and square conservative temporal integration scheme. In this study, we demonstrate that square conservation is equivalent to energy conservation in both a continuous shallow water system and a discrete shallow water system of TRiSK, attempting to extend the square conservation ~~theory~~ law to the TRiSK framework. To overcome the challenge of constructing an anti-symmetrical spatial discrete operator, we unify the unit of evolution variables of shallow water equations by Institute of Atmospheric Physics (IAP) transformation, ~~expressing the temporal trend of the evolution variable by using the original operators of TRiSK~~ the temporal derivates of new evolution variables can be expressed by a combination of temporal derivates of original evolution variables, which means the square conservative spatial discrete operator can be obtain by using original spatial discrete operator in TRiSK. Using the square conservative Runge-Kutta scheme, the total energy is completely conserved, and there is no influence on the properties of conserving total mass and total absolute vorticity. In the standard shallow water numerical test, the square conservative scheme not only helps maintain total conservation of the three integral invariants but also creates less simulation error norms.

1 Introduction

In a statistical sense, ~~The~~ the ~~maintenance of~~ integral constraints ~~is necessary to determine the true solution, following a path upon which the statistics are analogous to those of the true solution~~make the physics of the discrete model more analogous to the physics of the continuous atmosphere, and also make the errors less systematic (Arakawa, 1977). Shallow water equation sets, without any outer sources and frictions, have five basic physical conservation properties, including total mass, total energy, total absolute vorticity (total potential vorticity), total potential enstrophy and total angular momentum. These conservation properties are important in an atmosphere model, especially with regard to long-term simulation; however, in a discrete system, some conservation properties cannot be maintained (Wang, 2008). If the square of a quantity is conserved with time when summed up over all the grid points in a domain, the quantity itself will be bounded, at every individual grid point, throughout the entire period of integration, this might be helpful for preventing nonlinear computational instability (Arakawa, 1966), and energy is one kind of the quadratic quantities. Toy and Nair (2017) developed an energy and potential enstrophy conserving scheme for shallow water equations on generalized curvilinear coordinates, they mentioned conserving analogues of total energy and total potential enstrophy in numerical models are known to prevent a spurious cascade of energy toward small scales. For a short-term simulation, the influences of slight energy dissipation are not obvious, but this dissipation accumulates in every time step, and finally, in a long-term simulation, leads to a quiet different result, i.e., an ellipse orbit tends to a single point after 10^8 steps (Wang, 1996).

A numerical scheme, with an energy conservation or energy dissipative property, is prerequisite to prevent nonlinear computational instability; however, an energy dissipative scheme will limit short-waves, which ~~is~~are meaningful for the atmosphere (Shen, 2013; Zeng, 1981).

On a latitude–longitude grid, energy is able to be entirely conserved by constructing a square conservative finite difference scheme (Ji and Wang, 1991), or a multi-conservation finite difference scheme (Wang and Ji, 2003), the former of which is better developed. Wang and Ji (1994a) discussed the square conservative scheme (SCS), the complete square conservative scheme (CSCS), the instantaneous square conservative scheme (ISCS) and the explicit complete square conservative scheme with adjustable time intervals (ECSCSA). The ISCS maintains square conservation only in the spatial discrete scheme and not in the temporal integration scheme, which implies the spatial discrete operator of the model is a square conservative (i.e., an anti-symmetrical operator). However, the temporal integration scheme does not possess the square conservation property ~~because~~ therefore the model is energy dissipative during integration. The CSCS maintains square conservation in both the spatial and temporal schemes. The model, which adopts CSCS, is able to maintain complete energy conservation during integration. The first step of applying the square conservation theory is to construct an anti-symmetrical spatial discrete operator and then integrate the model with a square conservative temporal integration scheme, i.e., a modified predict-corrector, modified leap-frog (Wang and Ji, 2006), harmonious dissipative operators (Wang and Ji, 1994b), etc.

To improve integration precision on the temporal direction of the square conservative scheme, a new class of Runge-Kutta schemes, hereafter ~~CRK~~NRK, were developed by Wang et al. (1996). The ~~CRK~~NRK scheme maintains the complete square conservation property by adjusting the length of temporal integration steps and maintaining the same integral precision order as the original Runge-Kutta scheme, hereafter RK.

The SCS was implemented in the grid-point atmospheric model of IAP LASG (GAMIL, Wang et al. 2004, Wang and Ji, 2006). GAMIL is widely used in climate simulation (Li et al., 2007, 2013; Wu and Li, 2008). The square conservation theory is rarely used on quasi-uniform grids or nonuniform grids because it is hard to construct a spatial discrete operator with an anti-symmetrical property on those grids.

In the most recent two decades, to avoid the polar ~~problem~~ singularity of the latitude–longitude grid, increasingly more atmosphere models have been built on the quasi-uniform grid, i.e., spectral transform methods (Swarztrauber, 1996); the finite volume method (Lin, 2004; Putman and Lin, 2007; Chen and Xiao, 2008); and an extension on the finite difference method to the generalized curvilinear coordinates (Toy and Nair, 2017).

Thuburn et al. (2009) and Ringler et al. (2010), provided a spatial discrete scheme based on arbitrarily structured C-grids, known as Thuburn–Ringler–Skamarock–Klemp (TRiSK). TRiSK is able to conserve the total mass and total absolute vorticity, and the total energy is ~~instantaneously conserved~~conserved within time-truncation error. These important properties enable models using quasi-uniform Voronoi grids, the accuracies of which are similar to latitude–longitude grids (Weller et al., 2012). Based on Thuburn et al. (2009) and Ringler et al. (2010), a global/regional model, the Model for Prediction Across Scales (MPAS), was developed by the National Center for Atmospheric Research (NCAR) and Los Alamos National Laboratory (LANL) (Skamarock et al., 2012, 2018).

Although the ~~semi~~spatial- discrete operator designed by Ringler et al. (2010) results in ~~instantaneous~~ energy conservation~~conservation~~, the total energy is still dissipative while using dissipative temporal integration schemes, i.e., Runge-Kutta, in other words, the conservation property of spatial discrete operator is not able to be maintain during temporal integration, this is so-call conserving total energy in time truncation error. In this paper we attempt to construct a square conservative scheme for TRiSK, which is able to conserve total energy in round-off error, but not just in time truncation error, which means that the variation of total energy should be in round-off error during entire temporal integration period, we call this complete energy conservation.~~Energy will be completely conserved only when the spatial discrete operator is anti-symmetrical and the temporal integration scheme is square conservative (Wang and Ji, 2006).~~

Total Energy will be completely conserved only if the spatial discrete operator is anti-symmetrical and the temporal integration scheme is square conservative (Wang and Ji, 2006). The main obstacle of extending square conservation to the quasi-uniform grids is constructing the anti-symmetrical spatial discrete operator. Because many quasi-uniform grids are unstructured and the shapes of cells are not uniform, it is difficult to find the next or previous cell. In this study, we use the instantaneous energy conservation property of TRiSK to overcome the challenge of constructing an anti-symmetrical spatial operator on a quasi-uniform grid. After using ~~CRK~~NRK as a temporal integration scheme, the square conservative constrains are satisfied for both spatial and temporal directions, and the total energy, total mass and total absolute vorticity are completely conserved during the integration.

This paper is presented as follows: In section 2, we review the TRiSK framework which was described by Ringler et al. (2010). Section 3 describes the method of extending square conservation to TRiSK in 3 parts. The first part presents a review of square conservation and a demonstration of the equivalent relationship between square conservation and energy conservation in a continuous shallow water system. In the second part of section 3, we obtain the anti-symmetrical spatial discrete operator by using the derivative rule and the energy conservation property of TRiSK, a method that is key to extending square conservation to TRiSK. In the last part of section 3, we review a new type of Runge-Kutta with 4th-order precision, which was developed by Wang et al. (1996) as the square conservative temporal integration scheme. In section 4, by using the square conservation scheme, we demonstrate that the total mass and total absolute vorticity remain perfectly conservative. Section 5 exhibits the results of three different numerical tests, including the 2nd, 5th and 6th test cases mentioned by Williamson (1992).

2 Introduction of TRiSK

The shallow water equation set may be written in a vector-invariant~~flux~~ form~~at~~ as follows:

$$\frac{\partial \boldsymbol{u}}{\partial t} - \xi_a \boldsymbol{k} \times \boldsymbol{u} + \nabla E = 0\,, \tag{1}$$

$$\frac{\partial \phi}{\partial t} + \nabla \cdot (\phi \boldsymbol{u}) = 0\,, \tag{2}$$

where, $\xi_a = \xi + f$ denotes the absolute vorticity; $\xi = \nabla \times \boldsymbol{u}$ represents the relative vorticity; $f = 2\Omega \sin\theta$ is the Coriolis parameter; $E = K + g(h + h_s) = K + \phi + \phi_s$, $\phi = gh$ is the geopotential depth of the fluid; $\phi_s = gh_s$ is the geopotential height of the underlying surface; $\phi_t = \phi + \phi_s$ is the free surface (top) of the fluid; $K = \frac{|\boldsymbol{u}|^2}{2}$ is the kinetic energy; $\boldsymbol{u}$ is the velocity vector; h and h_s are the fluid thickness and surface height, respectively; θ represents the latitude; and g and Ω are acceleration of gravity and angular velocity of the earth.

In Ringler et al. (2010), the total energy is defined as

$$\epsilon_{R10} = hK + gh\left(\frac{1}{2}h + h_s\right)$$

To simplify the derivation in the following context, we define the total energy as

$$\oiint_\Omega \epsilon\, ds = \oiint_\Omega g\epsilon_{R10}\, ds = \oiint_\Omega \phi K + \frac{1}{2}\phi^2 + \phi\phi_s\, ds = \|\phi K\| + \left\|\frac{1}{2}\phi^2\right\| + \|\phi\phi_s\| \cancel{\epsilon = g\epsilon_{R10} = \phi K + \frac{1}{2}\phi^2 + \phi\phi_s = \|\phi K\| + \left\|\frac{1}{2}\phi^2\right\| + \|\phi\phi_s\|}\,, \tag{3}$$

where $\|\cdot\| = \sqrt{(\cdot,\cdot)}$ denotes the 2-norm. The inner product $(\cdot,\cdot)$ is defined as

$$(X, Y) = \oiint_\Omega X \cdot Y\, ds$$

where Ω is the entire spherical surface.

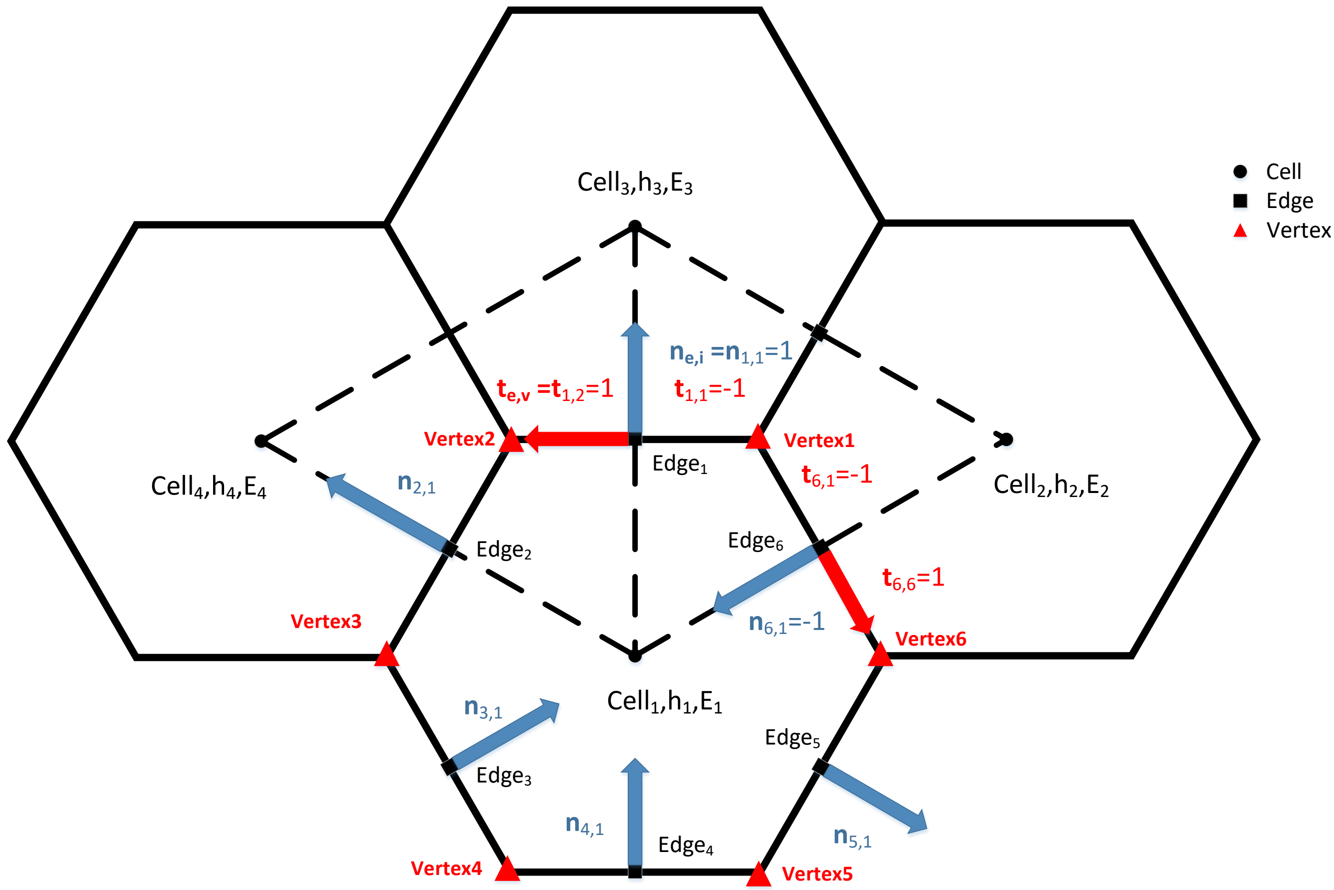

Figure 1. Definition of elements in a discrete system. Blue arrows represent the indicator function $\boldsymbol{n}_{e,i}$ and red arrows are the indicator function $\boldsymbol{t}_{e,v}$. The uniform grid is here for clearly introducing SCVT meshes, the situation on non-uniform grid is similar.

Per the description provided in Ringler et al. (2010), velocity points are on the edges of each cell, the mass and kinetic energy points are in the center of ~~the~~ each cell and vorticity points are on the vertices of ~~the~~ each cell. The shallow water equation set may be expressed as a ~~semi-~~discrete form:

$$\frac{\partial u_e}{\partial t} - Q_e^{\perp} + [\nabla E]_e = 0\,, \tag{4}$$

$$\frac{\partial \phi_i}{\partial t} + [\nabla \cdot (\phi u)]_i = 0\,, \tag{5}$$

where u_e~~, v~~, ϕ_i are the normal velocity and ~~tangent velocity~~geopotential height. The subscript e signifies that the variable is defined on edge e; the subscript i signifies that the variable is defined at the center of ith~~a~~ cell. $Q_e^{\perp}$ is the absolute vorticity flux on the tangent direction $\perp$ of the edge e, which is computed according to Eq. (49) in Ringler et al. (2010).

$$[\nabla E]_e = \frac{1}{d_e} \sum_{i \in CE(e)} -n_{e,i} E_i$$

$$[\nabla \cdot (\phi u)]_i = \frac{1}{A_i} \sum_{e \in EC(i)} n_{e,i} l_e \phi_e u_e$$

where $n_{e,i}$ is an indicator function, defined as $n_{e,i} = 1$ when n_e is an outward normal vector of cell i, and $n_{e,i} = -1$ when n_e is an inward normal vector of cell i; l_e is the length of edge e; $i \in CE(e)$ denotes the two cells that share edge e; and $e \in EC(i)$ is the set of edges that define the boundary of cell i. The potential vorticity on edge q_e may be computed by the midpoint method (Ringler et al. (2010), Eq. (50)) or the linear interpolation method (Weller, 2012, Eq. (5)). The details are presented in Figure 1.

3 Extending the square conservation to TRiSK

As mentioned in section 1, to obtain the complete square conservation property, the spatial discrete operator must be anti-symmetrical, and the temporal integration scheme is square conservative. Therefore, in this section, the method of extending the square conservation to TRiSK is introduced in three parts. Subsection 3.1 reviews the concept of square conservation, demonstrating the equivalent relationship between the square conservation and energy conservation. Subsection 3.2 constructs the anti-symmetrical spatial discrete operator. Subsection 3.3 introduces the square conservative temporal integration scheme by reviewing a ~~new type~~ class of Runge-Kutta (~~CRK~~NRK), which was developed by Wang et al. (1996).

3.1 Relationship between Square Conservation and Energy Conservation

First, we review the concept of anti-symmetrical operators and square conservation according to the study of Wang et al. (1996), considering the nonlinear evolution equation in operator form:

$$\frac{\partial \boldsymbol{F}}{\partial t} + \mathcal{L}(\boldsymbol{F}) = 0 \,, \tag{6}$$

Definition. Suppose H is a complete inner product space on R and $\mathcal{L}$ is an $H \to H$ operator; if $\mathcal{L}$ satisfies the following inner product equation

$$(\mathcal{L}(\boldsymbol{F}), \boldsymbol{F}) = 0 \,, \tag{7}$$

then $\mathcal{L}$ is termed an anti-symmetrical operator.

The result of multiplying F on both sides of (6) and integrating globally is the square conservation property:

$$\frac{d}{dt} \|\boldsymbol{F}\|^2 = 0 \,, \tag{8}$$

Next, we begin determine the relationship between energy conservation and square conservation. In the TRiSK framework, the evolution variables are $\boldsymbol{u}$ and ϕ.

The unified unit of evolution variables is the prerequisite of constructing the square conservation system. The evolution variables are unified by IAP transformation (Zeng and Zhang, 1987; Wang et. al, 2004), and the original evolution variable $\boldsymbol{u}$ is replaced by the new evolution variable $\boldsymbol{U} = \sqrt{\phi}\boldsymbol{u}$, after completing IAP transformation.

$$\boldsymbol{F} = \begin{pmatrix} \boldsymbol{U} \\ \phi \end{pmatrix} = \begin{pmatrix} \sqrt{\phi}\boldsymbol{u} \\ \phi \end{pmatrix}, \tag{9}$$

The physical significance of $\sqrt{\phi}$ is the phase speed of the external-gravity wave, and the shallow water equation set may be rewritten as a vector format:

$$\frac{\partial \boldsymbol{F}}{\partial t} + \mathcal{L}(\boldsymbol{F}) = \frac{\partial}{\partial t}\begin{pmatrix} \boldsymbol{U} \\ \phi \end{pmatrix} + \mathcal{L}\begin{pmatrix} \boldsymbol{U} \\ \phi \end{pmatrix} = 0\ , \tag{10}$$

As defined in section 2, $\phi_t = \phi + \phi_s$

$$\frac{\partial \phi_t}{\partial t} = \frac{\partial \phi}{\partial t} + \frac{\partial \phi_s}{\partial t}$$

The surface height is determined to be independent of time,

$$\frac{\partial \phi_s}{\partial t} = 0$$

Therefore,

$$\frac{\partial \phi_t}{\partial t} = \frac{\partial \phi}{\partial t}\ , \tag{11}$$

Defining $\boldsymbol{F}_t = \begin{pmatrix} \boldsymbol{U} \\ \phi_t \end{pmatrix}$, according to (9) and (11), we have

$$\frac{\partial \boldsymbol{F}_t}{\partial t} = \frac{\partial \boldsymbol{F}}{\partial t}\ , \tag{12}$$

Multiplying (12) by $\boldsymbol{F}_t$ on both sides, and integrating globally

$$\frac{d}{dt}\left\|\frac{1}{2}\boldsymbol{F}_t^2\right\| = \left(\boldsymbol{F}_t, \frac{\partial \boldsymbol{F}}{\partial t}\right)$$

$$= \oiint_{\Omega} \boldsymbol{U}\ \frac{\partial \boldsymbol{U}}{\partial t} + (\phi + \phi_s)\frac{\partial \phi}{\partial t}\, ds$$

$$= \oiint_{\Omega} \frac{\partial}{\partial t}\left(\frac{1}{2}|\boldsymbol{U}|^{\boldsymbol{2}}\right) + \frac{\partial}{\partial t}\left(\frac{1}{2}\phi^2 + \phi\phi_s\right) ds$$

$$= \frac{d}{dt}\left(\|\phi K\| + \left\|\frac{1}{2}\phi^2\right\| + \|\phi\phi_s\|\right)$$

$$= \frac{d\epsilon}{dt} = 0$$

Accordingly, square conservation is equivalent to energy conservation in a continuous system.

3.2 Constructing the anti-symmetrical spatial discrete operator

In this subsection, we construct the anti-symmetrical spatial discrete operator by a specific combination of original operators in TRiSK. Firstly, we need to demonstrate the equivalent relationship between square conservative spatial discrete operator and energy conservative spatial discrete operator in continuous system, then prove that this relationship is also apply to discrete system.

Assuming a continuous-in-time system, the evolution equation of $\boldsymbol{U}$ is able to be expressed as

$$\frac{\partial \boldsymbol{U}}{\partial t} = \sqrt{\phi}\frac{\partial \boldsymbol{u}}{\partial t} + \frac{\boldsymbol{u}}{2\sqrt{\phi}}\frac{\partial \phi}{\partial t}, \tag{13}$$

This formula is key to connecting square conservation and energy conservation; it is difficult to directly construct the anti-symmetrical operator on quasi-uniform grids.

Theorem. The ~~operators~~ functions $\mathcal{M} = \mathcal{M}(\phi, u)$ *and* $\mathcal{N} = \mathcal{N}(\phi, u)$ *satisfy*

$$\begin{cases} \frac{\partial \boldsymbol{u}}{\partial t} + \mathcal{M}\cancel{u} = 0 \\ \frac{\partial \phi}{\partial t} + \mathcal{N}\cancel{\phi} = 0 \end{cases}, \tag{14}$$

and

$$(\mathcal{M}\cancel{u}, \phi u) + (\mathcal{N}\cancel{\phi}, E) = 0$$

After IAP transformation (9), *the evolution equation of* $\boldsymbol{U}$ *may be expressed as* (13), *and* (14) *may be rewritten as* (10).

If the operator $\mathcal{L}$ *satisfies* (10), *then* $\mathcal{L}$ *is an anti-symmetrical operator.*

Proof.

$$\frac{\partial \boldsymbol{U}}{\partial t} = \sqrt{\phi}\frac{\partial \boldsymbol{u}}{\partial t} + \frac{\boldsymbol{u}}{2\sqrt{\phi}}\frac{\partial \phi}{\partial t} = -\sqrt{\phi}\mathcal{M}\cancel{u} - \frac{\boldsymbol{u}}{2\sqrt{\phi}}\mathcal{N}\cancel{\phi}$$

$$(\mathcal{L}(\boldsymbol{F}), \boldsymbol{F}) = -\left(\frac{\partial \boldsymbol{U}}{\partial t}, \boldsymbol{U}\right) \cancel{+} - \left(\frac{\partial \phi}{\partial t}, \phi\right)$$

$$= \oiint_{\Omega} -\boldsymbol{U}\frac{\partial \boldsymbol{U}}{\partial t} - \cancel{+}\phi\frac{\partial \phi}{\partial t}\, ds$$

$$= \oiint_{\Omega} -\boldsymbol{U}\left(-\sqrt{\phi}\mathcal{M}\cancel{u} - \frac{\boldsymbol{u}}{2\sqrt{\phi}}\mathcal{N}\cancel{\phi}\right) \cancel{-} + \phi\mathcal{N}\cancel{\phi}\, ds$$

$$= \oiint_{\Omega} \cancel{-}\phi u \cdot \mathcal{M}\cancel{u} + \cancel{-}\frac{|\boldsymbol{u}|^2}{2}\mathcal{N}\cancel{\phi} + \cancel{-}\phi\mathcal{N}\cancel{\phi}\, ds$$

$$= \cancel{-}(\mathcal{M}\cancel{u}, \phi u) + \cancel{-}(\mathcal{N}\cancel{\phi}, E)$$

$$= 0$$

This theorem is proved in a continuous system, but the model is built in a discrete system; therefore, it is necessary to discuss the situation in a discrete system.

Following Ringler et al. (2010), we set the discrete ~~operators~~ functions $M = M(\phi, u)$ and $N = N(\phi, u)$ as:

$$M\cancel{u} = [\nabla E]_e - Q_e^{\perp}$$

$N\cancel{\phi} = [\nabla \cdot (\phi u)]_i$

And the semi-discrete shallow water equation set becomes

$$\frac{\partial u}{\partial t} + M\cancel{u} = 0 \, , \qquad (15)$$

$$\frac{\partial \phi}{\partial t} + N\cancel{\phi} = 0 \, , \qquad (16)$$

Because the ~~semi-~~spatial discrete operator of TRiSK has an instantaneous energy conservation property, it is easy to prove $(M\cancel{u}, \phi u) + (N\cancel{\phi}, E) = 0$. (Details in Ringler et al. (2010), section 3.7.2)

There are cells, edges and vertices presented as three types of points on a spherical centroidal Voronoi tessellation (SCVT) grid, which is the mesh used by TRiSK. We define the inner product for different types of points as:

$(X, Y)_i = \sum_{i=1}^{nCells} X_i \cdot Y_i \cdot A_i$

$(X, Y)_e = \sum_{e=1}^{nEdges} X_e \cdot Y_e \cdot A_e$

where X_i, Y_i are the variables in the cell; X_e, Y_e denote any variables on the edge; A_i, A_e are the areas for each cell and edge; $A_e = d_e \times l_e$, d_e is the distance between the two cells' centers on edge e; l_e is the length of edge e; $nCells$ denotes the total cell number; and $nEdges$ is the total edge number.

$$\left(M\cancel{u}, \phi\cancel{(\widehat{\phi})_e}u\right)_e + (N\cancel{\phi}, E)_i = 0 \, , \qquad (17)$$

Combining (10) and (13), and rewriting into a discrete system

$$\frac{\partial \boldsymbol{F}}{\partial t} + L(\boldsymbol{F}) = \frac{\partial}{\partial t}\begin{pmatrix} U_e \\ \phi_i \end{pmatrix} + L\begin{pmatrix} U_e \\ \phi_i \end{pmatrix} = 0 \, , \qquad (18)$$

where $U_e = \sqrt{\phi_e}u_e$, $\sqrt{\phi_e}$ is the phase speed of external-gravity wave on edge e. Note we need to interpolate ϕ_i from cell center i to edge e, here we set $\phi_e = \frac{1}{2}\sum_{i \in CE(e)} \phi_i$.

$$\frac{\partial U_e}{\partial t} = \sqrt{\phi_e}\frac{\partial u_e}{\partial t} + \frac{u_e}{2\sqrt{\phi_e}}\frac{\partial \phi_e}{\partial t} = -\sqrt{\phi_e}M\cancel{u} - \frac{u_e}{2\sqrt{\phi_e}}N\cancel{\phi} \, , \qquad (19)$$

As shown in the Appendix A, we have the discrete anti-symmetrical operator L

$$(L(\boldsymbol{F}), \boldsymbol{F})_d = -\left(U, \frac{\partial U}{\partial t}\right)_e - \cancel{+}\left(\phi, \frac{\partial \phi}{\partial t}\right)_i = 0 \, , \qquad (20)$$

The subscript d represents that the inner product is computed in a discrete system.

Thus, the discrete evolution equation set becomes

$$\frac{\partial U_e}{\partial t} + \sqrt{\phi_e}M\cancel{u} + \frac{u_e}{2\sqrt{\phi_e}}N\cancel{\phi} = 0 \, , \qquad (21)$$

$$\frac{\partial \phi_i}{\partial t} + N\phi = 0 \ , \tag{22}$$

The model will be instantaneous square conservative by incorporating (21) and (22) as the evolution equation set.

3.3 Constructing the temporal integration scheme with the square conservation property

The model is integrated in a discrete-in-time system, for the sake of guaranteeing complete square conservation, a square conservative temporal integration scheme is necessary. As ~~CRK~~NRK has the advantage of maintaining complete square conservation with a high order of integral precision, the 4th-order ~~CRK~~NRK scheme in TRiSK is adopted to obtain high integral precision and a long-time step. To completely introduce the square conservative temporal integration scheme, we review some ~~of the~~ details in Wang et al. (1996).

The 4th-order ~~CRK~~NRK may be expressed as

$$F^{n+1} = F^n + \tau_n \varphi(F^n, \tau) \ , \tag{23}$$

where τ_n is an adjustable time step and τ is the integral time step of the model.

$$\varphi(F^n, \tau) = \tau \frac{R_1 + 2R_2 + 2R_3 + R_4}{6}$$

$$\begin{cases} R_1 = -LF^n \\ R_2 = -L\left(F^n + \frac{1}{2}\tau R_1\right) \\ R_3 = -L\left(F^n + \frac{1}{2}\tau R_2\right) \\ R_4 = -L(F^n + \tau R_3) \end{cases}$$

Taking square operators on both sides of (23), delineating $\varphi^n = \varphi(F^n, \tau)$

$$\|F^{n+1}\|^2 = \|F^n\|^2 + 2\tau_n(\varphi^n, F^n) + {\tau_n}^2 \|\varphi^n\|^2 \ , \tag{24}$$

We notice that although the spatial discrete operator L is anti-symmetrical, the total energy at the $n+1$ time point remains different from that at the n time point. Energy is able to be completely conserved by satisfying the following equation:

$$\|F^{n+1}\|^2 = \|F^n\|^2$$

Therefore,

$$2\tau_n(\varphi^n, F^n) + {\tau_n}^2 \|\varphi^n\|^2 = 0$$

$$\tau_n = -\frac{2(\varphi^n, F^n)}{\|\varphi^n\|^2}$$

Considering the fitness when $\tau \to 0$, as described in Eqs. (17)–(18) in Wang et al. (1996)

$$\tau_n = \frac{\tau}{3\|\varphi^n\|^2}\left[(R_1, R_2) + (R_2, R_3) + (R_3, R_4)\right] \ , \tag{25}$$

Once adopting the ~~CRK~~NRK scheme as the temporal integration scheme, the model will be completely square conservative, which implies the total energy will be completely conserved from the beginning to the end of the integration. The ~~CRK~~NRK scheme is expected to perform better than RK in a numerical test. Moreover, ~~CRK~~NRK decays to RK by setting $\tau_n = \tau$.

While the integral time step is modified from τ to τ_n, the precision order of ~~CRK~~NRK is the same as RK, when constructing ~~CRK~~NRK based on the nth order RK, ~~CRK~~NRK has nth order precision either, a conclusion proven by Theorem 1 in Wang et al. (1996).

4 Mass and Absolute Vorticity Conservation

In the CSCS introduced above, although the integral time step is modified from τ to τ_n, the total mass and total absolute vorticity are nevertheless conserved. In the following demonstrations, we notice that the mass conservation property and absolute vorticity conservation property are independent of temporal integration.

4.1 Mass Conservation

Considering the total mass, multiplying (5) by A_i and summing all cells,

$$\sum_{i=1}^{nCells} A_i \frac{\partial \phi_i}{\partial t} = -\sum_{i=1}^{nCells} A_i [\nabla \cdot (\phi u)]_i = -\sum_{i=1}^{nCells} \sum_{e \in EC(i)} n_{e,i} l_e \phi_e u_e = -\sum_{e=1}^{nEdges} \sum_{i \in CE(e)} n_{e,i} l_e \phi_e u_e = -\sum_{e=1}^{nEdges} l_e \phi_e u_e - l_e \phi_e u_e = 0$$

Notice that the mass conservation property is independent of temporal integration.

4.2 Absolute Vorticity Conservation

According to Ringler et al. (2010) formula (23), the relative vorticity is calculated according to the following diagnostic equation:

$$\xi = \frac{1}{A_v} \sum_{e \in EV(v)} t_{e,v} u_e d_e$$

Multiplying by A_v and summing all of the vertices yields

$$\sum_{v=1}^{nVertices} A_v \xi = \sum_{v=1}^{nVertices} \sum_{e \in EV(v)} t_{e,v} u_e d_e = \sum_{e=1}^{nEdges} \sum_{v \in VE(e)} t_{e,v} u_e d_e = \sum_{e=1}^{nEdges} u_e d_e - u_e d_e = 0$$

where $e \in EV(v)$ represents the set of edges that share the vertex v; $v \in VE(e)$ are the two vertices on edge e. The indicator function $t_{e,v}$ always points to the left side of $n_{e,i}$. If $\boldsymbol{k} \times n_{e,i}$ is directed toward vertex v, then $t_{e,v} = 1$; otherwise, $t_{e,v} = -1$. $\boldsymbol{k}$ is the unit vector, which points in the local vertical direction. See Figure 1 for details. The total relative vorticity is shown to always be zero and independent of time.

Another method to compute the relative vorticity is to use the following prognostic equation, as described in Ringler et al. (2010) Eq. (33)

$$\frac{\partial \xi}{\partial t} + \frac{1}{A_v} \sum_{e \in EV(v)} -t_{e,v} Q_e^{\perp} d_e = 0$$

Multiplying the above equation by A_v and summing all the vertices yields

$$\sum_{v=1}^{nVertices} A_v \frac{\partial \xi}{\partial t} = \sum_{v=1}^{nVertices} \sum_{e \in EV(v)} t_{e,v} Q_e^{\perp} d_e = \sum_{e=1}^{nEdges} \sum_{v \in VE(e)} t_{e,v} Q_e^{\perp} d_e = \sum_{e=1}^{nEdges} Q_e^{\perp} d_e - Q_e^{\perp} d_e = 0$$

Therefore, the relative vorticity is conserved during temporal integration.

Taking the partial derivative of the absolute vorticity with time yields

$$\frac{\partial \xi_a}{\partial t} = \frac{\partial \xi}{\partial t} + \frac{\partial f}{\partial t}$$

The Coriolis parameter is independent of time, $\frac{\partial f}{\partial t} = 0$; thus

$$\sum_{v=1}^{nVertices} A_v \frac{\partial \xi_a}{\partial t} = 0$$

5 Numerical Tests

To test the square conservation schemes using TRiSK, a new TRiSK-based shallow water dynamic core is developed, which is named TRiSK-based Multiple-Conservation dynamical cORE (TMCORE). The spatial discrete operators are the same as those introduced by Ringler et al. (2010), the evolution variable u_e is replaced by U_e, as we described above, and the temporal integration scheme is selected from RK or ~~CRK~~NRK, both of which are in 4th-order precision.

We expected that the square conservation scheme will work on arbitrarily structured C-grids with a different initial field and mesh of a different resolution. In this section, we test the new scheme by using standard shallow water test cases 2, 5 and 6 (SWTC2, SWTC5, SWTC6) with two different meshes, as presented by Williamson (1992). The first mesh has 2562 Voronoi cells (x1.2562), with an approximate resolution of 480 km, and the second mesh contains 40962 Voronoi cells (x1.40962), with an approximate resolution of 120 km. The corresponding integral time steps to x1.2562 and x1.40962 are 900 s and 360 s. Here, the midpoint scheme is selected as the method for interpolating the potential vorticity from vertices to edges for all tests.

In all of the test cases, we expect the complete energy conservation scheme (NRK) is able to conserve total mass, total absolute vorticity and total energy in round-off error, meanwhile, it would be even better if NRK can bring us less simulation error. Note, total energy is not merely conserved in time truncation error anymore, we need the change ratio of total energy to be limited in at least 10^{-14} magnitude.

5.1 Error measure methods

Global invariants error measure:

$$I(X^n) = \frac{S(X_i^n) - S(X_i^0)}{S(X_i^{\cancel{n}0})}$$

where X_i^n is the variable at the nth time point on the ith cell and X_i^0 is the variable at the initial time. The I function is the change ratio of the invariants.

The total mass error measure:

$$X_i^n = h_i^n$$

$$Mass\ Change\ Ratio = I(h^n)$$

The total energy error measure:

$X_i^n = \epsilon_i^n$

$Energy\ Change\ Ratio = I(\epsilon^n)$

Measuring the fluid thickness error by L_2 and L_∞ error norms is expressed as

$$L_2 = \frac{\left\{S\left[\left(f_m(i) - f_R(i)\right)^2\right]\right\}^{\frac{1}{2}}}{[S(f_R(i)^2)]^{\frac{1}{2}}}$$

$$L_\infty = \frac{\max|f_m(i) - f_R(i)|}{\max|f_R(i)|}$$

where i denotes the index of each cell; $f_m(i)$ and $f_R(i)$, respectively, are the model solution and reference solution at the ith cell on the mesh; and the S function is the area-weighted accumulation of an arbitrary variable X.

$$S(X) = \frac{\sum_{i=1}^{N} X(i)A(i)}{\sum_{i=1}^{N} A(i)}$$

where $A(i)$ is the area of the ith cell.

The reference solution should be an analytical solution or, when an analytical solution is not available, a high-resolution solution from the model with sufficient accuracy.

In the following context, ~~CRK4~~ NRK4 represents the ~~CRK~~NRK with 4th-order precision and RK4 represents the original Runge-Kutta scheme with 4th-order precision.

The differences of the error norms between ~~CRK4~~NRK4 and RK4 schemes by using the different ratios of L_2 (L2DR) and L_∞ (LInfDR) is expressed as:

$$L2DR = \frac{L_{2_{CRK4}} - L_{2_{RK4}}}{L_{2_{RK4}}}$$

$$LInfDR = \frac{L_{\infty_{CRK4}} - L_{\infty_{RK4}}}{L_{\infty_{RK4}}}$$

where $L_{2_{CRK4}}$ and $L_{2_{RK4}}$ are the L_2 error norms of ~~CRK4~~NRK4 and RK4, respectively, which is similar for $L_{\infty_{CRK4}}$ and $L_{\infty_{RK4}}$. ~~CRK4~~NRK4 has better performance than RK4 when the different ratios are negative; otherwise, ~~CRK4~~NRK4 has worse performance than RK4.

5.2 Global Steady State Nonlinear Zonal Geostrophic Flow (SWTC2)

For the Global Steady State Nonlinear Zonal Geostrophic Flow test case, the initial velocity field has the following form

$u = u_0 \cos\theta$

$v = 0$

The geopotential height field is

$$gh = gh_0 - \left(a\Omega u_0 + \frac{u_0^2}{2}\right)\sin^2\theta$$

Here, we set $\Omega = 7.292 \times 10^{-5}\, s^{-1}, g = 9.80616\, m/s^2, a = 6.37122 \times 10^6\, m, gh_0 = 2.94 \times 10^4\, m^2/s^2$ and $u_0 = 2\pi a/(12\ days)$, where h is fluid thickness, θ denotes latitude. In this test case, the exact solution is the initial state, and any difference between the numerical solution and the initial state is the simulation error.

In SWTC2, the true solution of $\frac{\partial u}{\partial t}, \frac{\partial v}{\partial t}, \frac{\partial \phi}{\partial t}$ is always zero; therefore, this test case can only represent the precision of spatial discrete operators but not the precision of temporal integration. This simulation is integrated for 10 years, but the shape of geostrophic flow breaks after 7 years. Therefore, we choose the simulation results from the 1st to the 7th year to compare the error norms of ~~CRK4~~NRK4 and RK4.

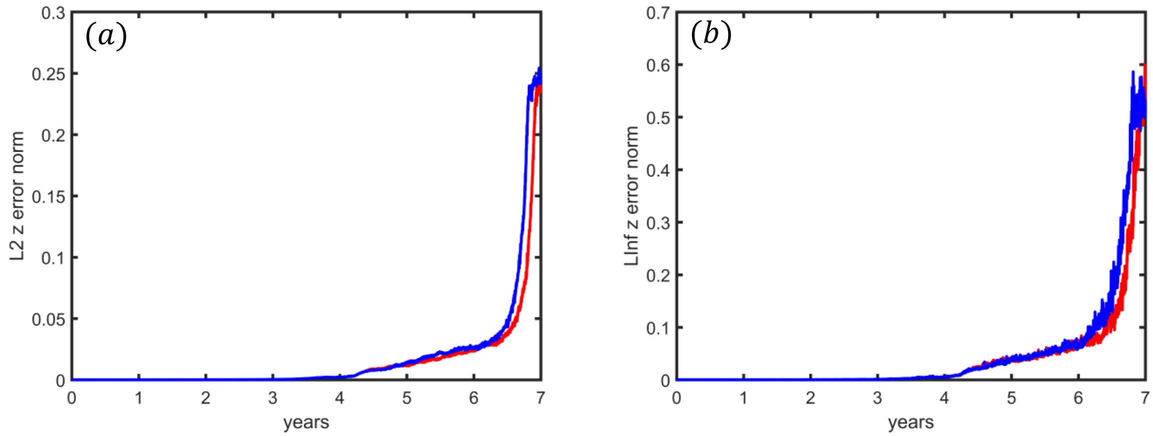

Figure 2. Geopotential height error norms of SWTC2. (a) $\mathbf{L_2}$ error norm; (b) $\mathbf{L_\infty}$ error norm. The results of RK4 and ~~CRK4~~NRK4 are represented by blue and red lines, respectively. The model mesh is x1.2562.

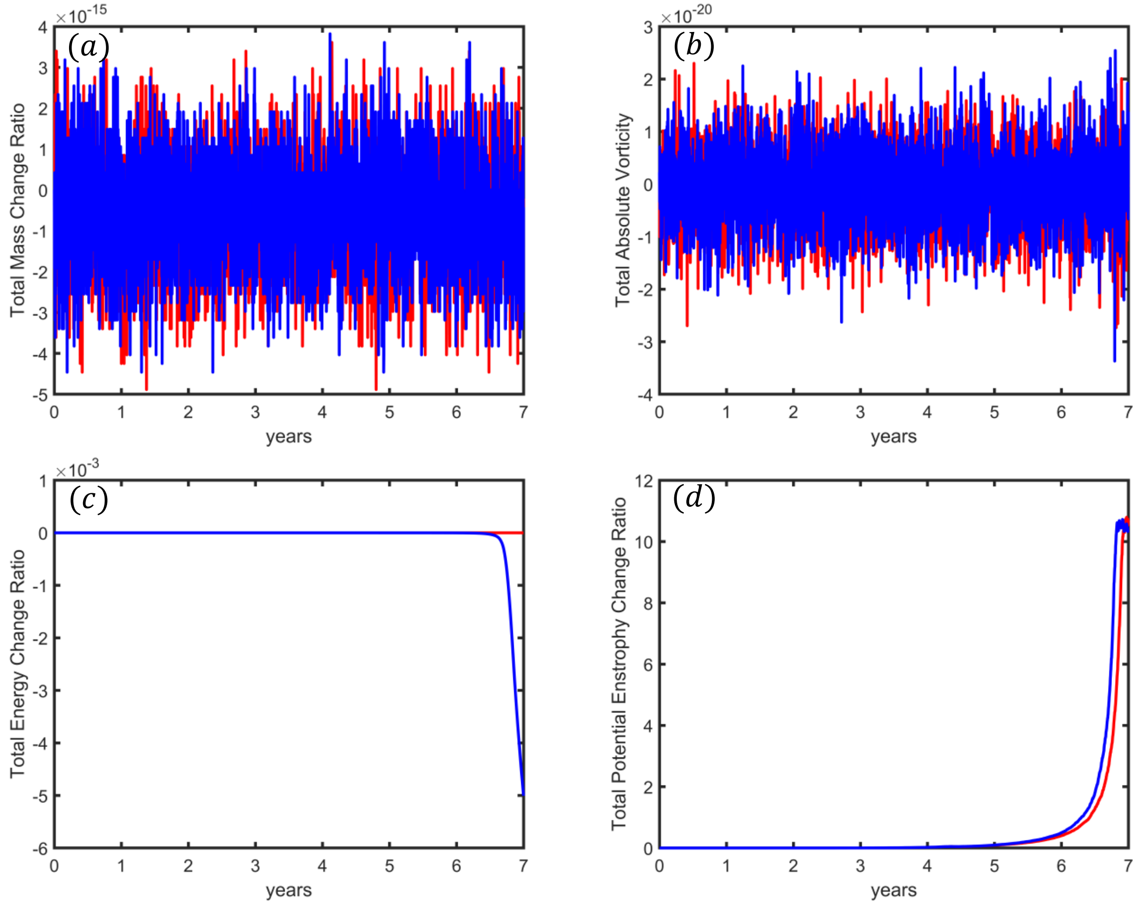

Figure 3. The variation of integral invariants as a function of time of SWTC2. (a) Total mass change ratio; (b) total absolute vorticity; (c) total energy change ratio; (d) total potential enstrophy change ratio. The results of RK4 are represented by blue lines; the results of ~~CRK4~~NRK4 are represented by red lines. The model mesh is x1.2562.

Figure 2 measures the L_2 and L_∞ error norms of geopotential height. In the first 4 years, the ~~CRK4~~NRK4 and RK4 exhibit similar results, but in the last 3 years, the shape of geopotential flow tends to break. The error norms increase sharply after 6 years, and the differences between ~~CRK4~~NRK4 and RK4 become more evident. Both the L_2 and L_∞ error norms of ~~CRK4~~NRK4 are evidently smaller than RK4, and the collapse of geopotential flow is delayed approximately 1 month when using ~~CRK4~~NRK4.

Figure 3 presents the variation of invariants as a function of time. ~~The oscillations of total mass and total absolute vorticity are strictly conserved.~~The change ratio of total mass is limited in 10^{-15} magnitude, and total absolute vorticity is oscillating around 10^{-20} magnitude, which means these two invariants are strictly conserved. The total energy of RK4 decreased approximately 0.5% in the final year, but ~~CRK4~~NRK4 maintains strict energy conservation (in 10^{-15} magnitude). Although the geopotential flow has been broken, ~~CRK4~~NRK4 prevents an increasing rate of total potential enstrophy.

5.3 Zonal Flow Over an Isolated Mountain (SWTC5)

SWTC5 is the 5th test case described by Williamson 1992; the wind and height fields are similar to SWTC2, but $h_0 = 5960\ m, u_0 = 20\ m/s$ and mountain height is determined according to the following equation:

$h_s = h_{s0}\left(1 - \frac{r}{R}\right)$

where $h_{s0} = 2000\ m$; $R = \frac{\pi}{9}$; $r = \sqrt{min[R^2, (\lambda - \lambda_c)^2 + (\theta - \theta_c)^2]}$; and λ_c and θ_c are the center longitude and latitude of the mountain, respectively. Here, we set $\lambda_c = \frac{3\pi}{2}$ and $\theta_c = \frac{\pi}{6}$. As the analytical solution is not available, the reference solution is provided by a T511 idealized global spectral atmospheric model from GFDL, where $8 \times 10^{12}\ m^4/s$ is selected as the coefficient for the ∇^4 dissipation, and the test case is integrated for 50 days.

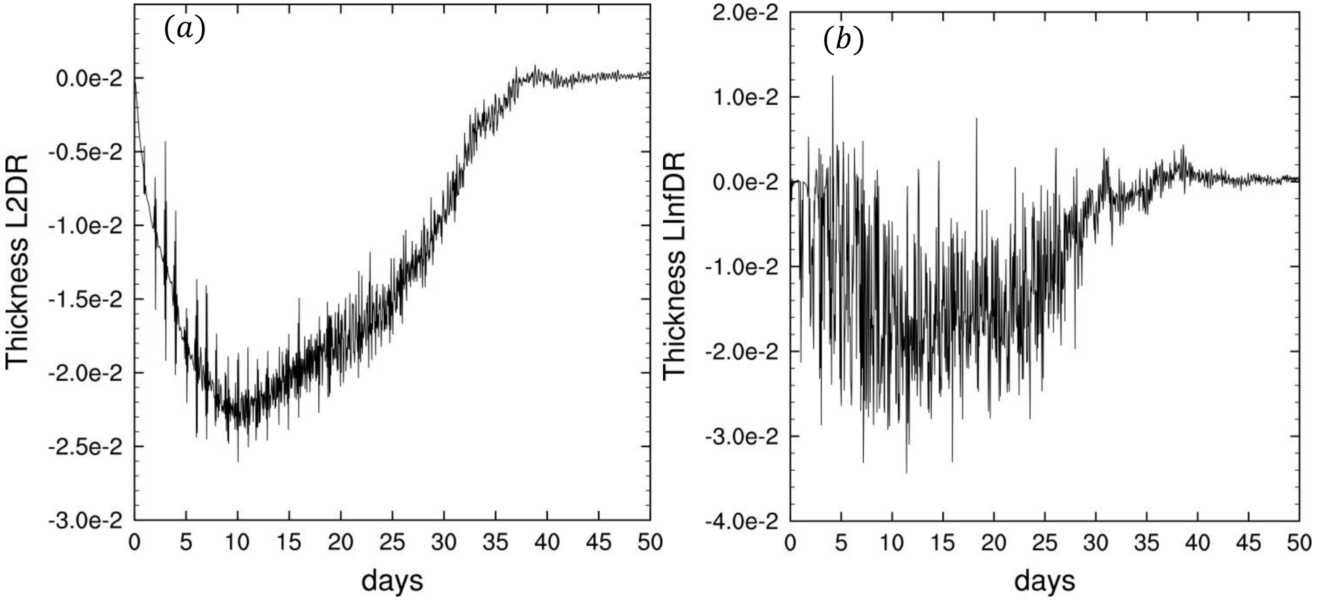

Figure 4. Fluid thickness error norms of different SWTC5 ratios. (a) $\mathbf{L_2}$ error norm difference ratio; (b) $\mathbf{L_\infty}$ error norm difference ratio. The model mesh is x1.40962.

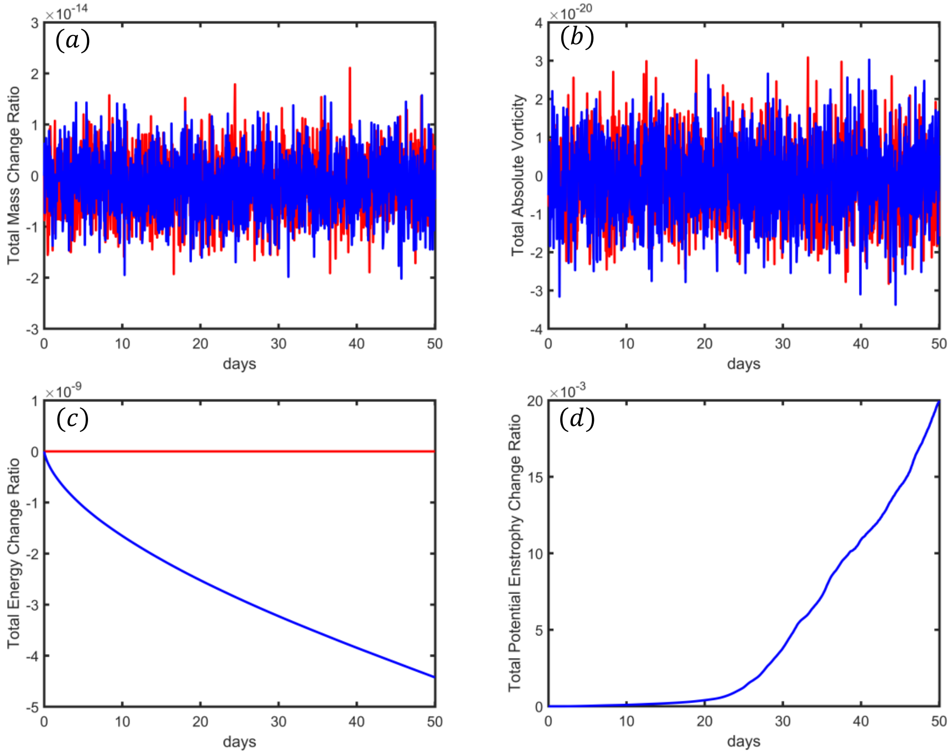

Figure 5. Integral invariants of SWTC5. (a) Total mass change ratio; (b) total absolute vorticity; (c) total energy change ratio; (d) total potential enstrophy change ratio. The results of RK4 and ~~CRK4~~NRK4 are represented by blue and red lines, respectively. The model mesh is x1.40962.

Figure 4 presents the different ratios of error norms. In the first 35 days, the L_2 and L_∞ error norms of ~~CRK4~~NRK4 are considerably smaller than those of RK4. Compared with RK4, the L_2 error norm of ~~CRK4~~NRK4 decreases by approximately 2.5% at the minimum point of L2DR, and the L_∞ error norm also decreases by approximately 3% at the minimum point of LInfDR. The error norms increase very quickly after 35 days; therefore, the differences between error norm ratios for ~~CRK4~~NRK4 and RK4 tend to be similar, along with time.

Figure 5 presents the variation of the invariants as a function of time. The total mass and total absolute vorticity are completely conserved for both ~~CRK4~~NRK4 and RK4. ~~CRK4~~NRK4 is able to maintain strict energy conservation (in 10^{-15} magnitude) from the beginning to the end, but the total energy of RK4 is dissipative. The CSCS exhibits no influence on the total potential enstrophy.

5.4 Rossby-Haurwitz Wave (SWTC6)

The classical 4 zonal wavenumber Rossby-Haurwitz wave was selected as the third test case. The initial condition follows Williamson (1992). The initial state is the analytical solution of the nonlinear barotropic vorticity equation on the sphere but not the analytical solution of the shallow water equations. The reference field is provided by a T511 idealized global spectral atmospheric model from GFDL. To limit the noise of the spectral model, we use $5 \times 10^{12}\ \mathrm{m}^4/s$ as the coefficient for the ∇^4 dissipation. As presented by Williamson, 1992, the phase speed of the Rossby-Haurwitz wave is calculated as follows:

$$c = \frac{R(R+3)\omega - 2\Omega}{(R+1)(R+2)}$$

where $R = 4$ is the zonal wavenumber of the Rossby-Haurwitz wave; $\omega = 7.848 \times 10^{-6} s^{-1}$; and $\Omega = 7.292 \times 10^{-5}\ s^{-1}$ is the rotation rate of the earth; therefore, the 4 zonal wavenumber period of the Rossby-Haurwitz wave is approximately 29.52 days. We integrate the test case over one period (33 days).

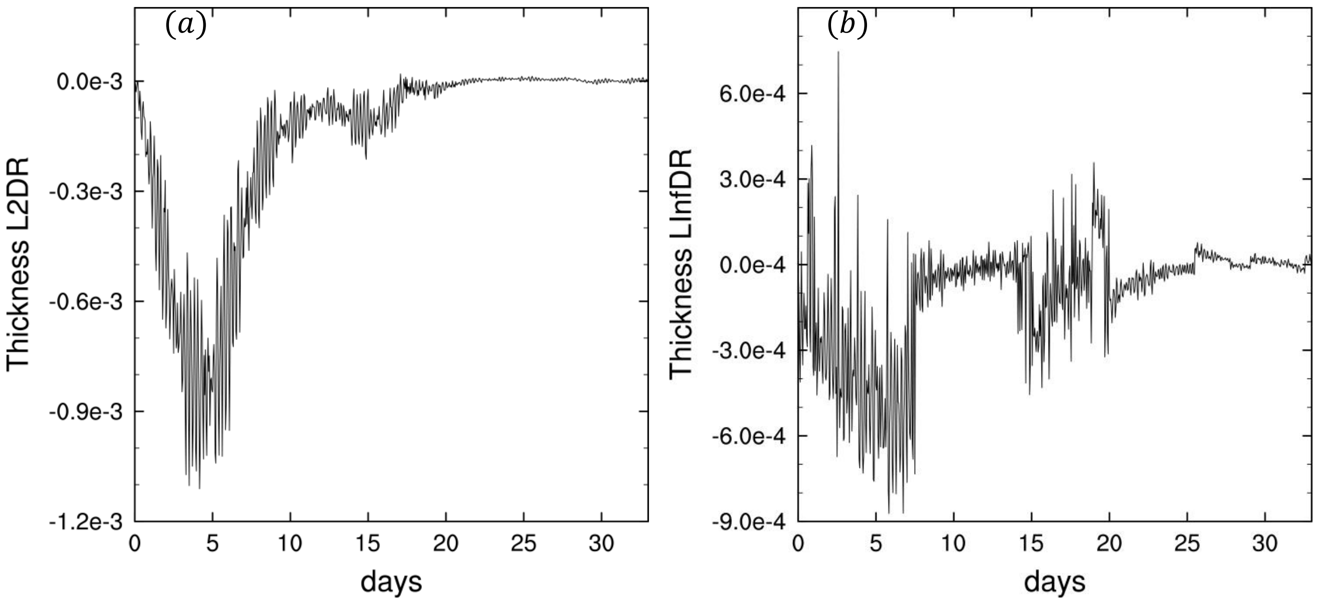

Figure 6. The fluid thickness error norms of different SWTC6 ratios. (a) L_2 error norm difference ratio; (b) L_∞ error norm difference ratio. The model mesh is x1.40962.

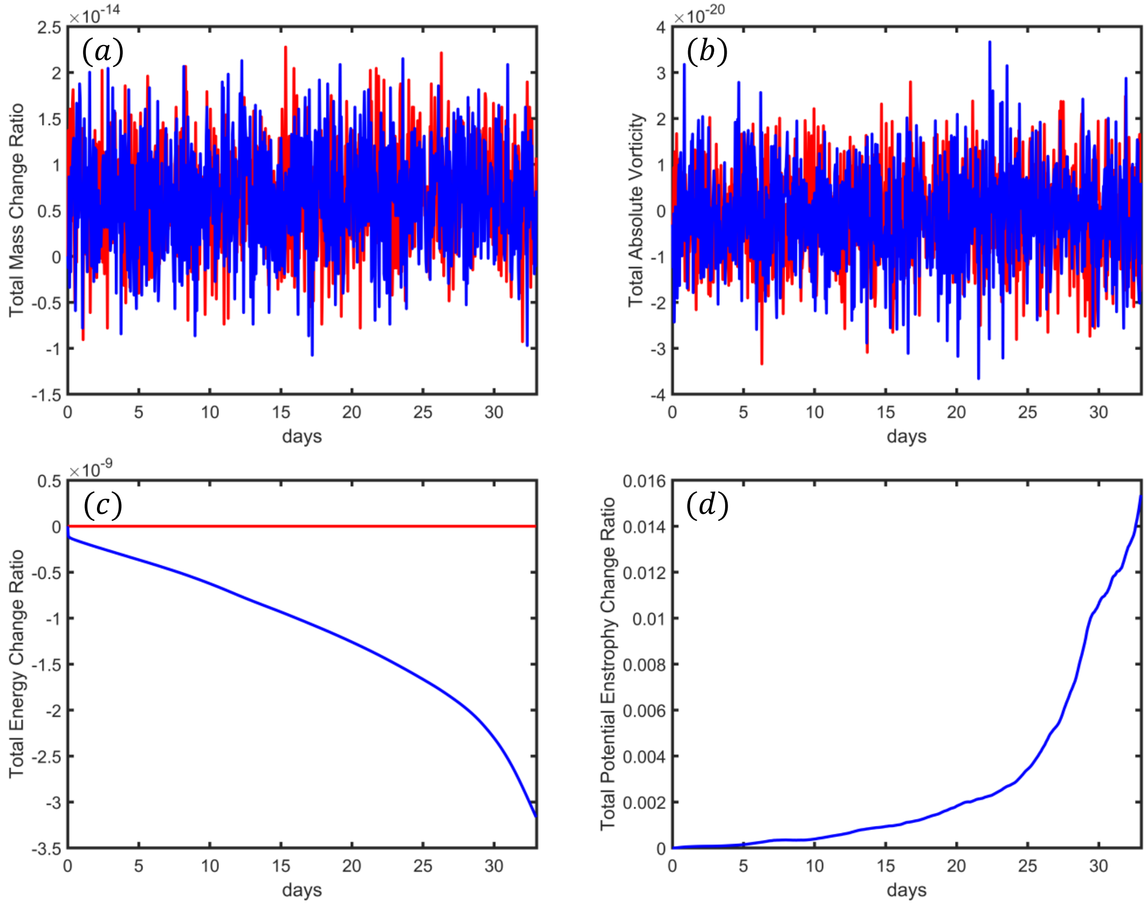

Figure 7. Integral invariants of SWTC6. (a) Total mass change ratio; (b) total absolute vorticity; (c) total energy change ratio; (d) total potential enstrophy change ratio. The results of RK4 and ~~CRK4~~NRK4 are represented by blue and red lines, respectively. The model mesh is x1.40962.

In both simulations of ~~CRK4~~NRK4 and RK4, the Rossby-Haurwitz wave begins to distort at the 25th day and then collapse a few days later.

Figure 6 presents the error norm difference ratios. ~~CRK4~~NRK4 has a smaller L_2 error norm than RK4 in the first 20 days. With growth of the L_2 error norm, the difference between ~~CRK4~~NRK4 and RK4 trends toward zero. At the 4th day, the L_2 error norm of ~~CRK4~~NRK4 is more than 0.11% less than that of RK4. ~~CRK4~~NRK4 also has a smaller L_∞ error norm a majority of the time. At the 6th day, the L_∞ error norm of ~~CRK4~~NRK4 is more than 0.08% less than that of RK4.

Figure 7 presents the variation of invariants as a function of time. The total mass and total absolute vorticity are strictly conserved for both ~~CRK4~~NRK4 and RK4. As expected, ~~CRK4~~NRK4 maintains strict energy conservation (in 10^{-15} magnitude), and RK4 cannot conserve the total energy during integration. With the Rossby-Haurwitz wave collapse, the total energy of RK4 rapidly dissipates after 25 days. There is no influence of ~~CRK4~~NRK4 to potential enstrophy in this case.

The red lines and blue lines in Figure 3c, Figure 5, Figure 7c are exactly the results of two kinds of energy conservation scheme, the blue lines present the property of conserving energy in time truncation error, and the red lines show conserving energy in round-off error, it's clear to see differences. As we mentioned above, conserving total energy in time truncation error leads to slightly energy dissipative, but the dissipate accumulates during integration, total energy may become zero after a long-term simulation, which is unreasonable for a pure dynamic core without any energy sink and source. On the other hand, complete energy conservation scheme maintains strictly energy conservation in entire integration period, even though it is not able to prevent the collapse of SWTC2, the collapse time is delayed, meanwhile, the simulation errors in SWTC5 and SWTC6 are reduced even if in a short-term simulation.

6 Summary

In this paper, we extend the CSCS to arbitrarily structured C-grids with shallow water equations, and we estimate the performance of the CSCS by using standard shallow water test cases.

There are two prerequisites for constructing CSCS, the anti-symmetrical spatial discrete operator and the square conservative temporal integration scheme. It is difficult to directly construct an anti-symmetrical spatial discrete operator on quasi-uniform grids; therefore, we take advantage of the instantaneous energy conservation property of the spatial discrete operators, as described by Ringler et al. (2010), to obtain the anti-symmetrical operator. After the IAP transformation, the units of evolution variables are unified, and the evolution variable u_e is replaced with $U_e = \sqrt{\phi_e} u_e$. According to the derivative rule (19), the temporal trend of U_e is expressed as a combination of the temporal trends of u_e and ϕ_i, and we demonstrate that the spatial discrete operator of U_e is an anti-symmetrical operator. Then, we integrate the model with the square conservative temporal integration scheme ~~CRK4~~NRK4, and the complete square conservation property is achieved.

An important finding is the equivalency between the energy conservative operator and anti-symmetrical operator for both the continuous system and discrete system. In most of previous study, anti-symmetrical operators were constructed on uniform grids, especially longitude–latitude grids, and the equation's advection term was in the advection-flux form. We extend the square conservation theory to a more general situation. The anti-symmetrical spatial discrete operator is constructed on quasi-uniform grids, and the equation is in the vector-invariant form.

The CSCS is able to maintain three integral invariants, including total mass, total absolute vorticity and total energy, in all the test cases, and the error norms decrease in varying degrees. The square conservation scheme improves the stability in SWTC2, and the error norms of ~~CRK4~~NRK4 are evidently less than RK4 after 4 years of simulation. For RK4, the total energy dissipates very quickly after the geostrophic flow collapse, but ~~CRK4~~NRK4 maintains complete energy conservation for the entire period, and the increasing rate of the total potential enstrophy is also limited by the square conservation scheme. In both SWTC5 and SWTC6, ~~CRK4~~NRK4 not only maintains strict conservation for three integral invariants but also leads to less error norms than RK4.

Appendix A

In this appendix, we attempt to demonstrate that the spatial discrete operator L is energy conservative. Our objective is to prove that the following equation is able to be satisfied by L,

$$\left(U,\frac{\partial U}{\partial t}\right)_e \cancel{=} + \left(\phi,\frac{\partial \phi}{\partial t}\right)_i = 0$$

Consider the inner product on edge

$$\left(U,\frac{\partial U}{\partial t}\right)_e = \sum_{e=1}^{nEdges} U_e \frac{\partial U_e}{\partial t} A_e$$

Substituting (19) into above formula

$$\left(U,\frac{\partial U}{\partial t}\right)_e = \sum_{e=1}^{nEdges} U_e \left(C_e \frac{\partial u_e}{\partial \mathrm{t}} + \frac{u_e}{2C_e\cancel{h_e}} \frac{\partial \phi_e}{\partial \mathrm{t}}\right) A_e$$

Where $C_e = \sqrt{\phi_e}$ is the phase speed of external-gravity wave on edge~~s~~ e.

According to Eq. (52) in Ringler et al. (2010),

$$\left(U,\frac{\partial U}{\partial t}\right)_e = \sum_{e=1}^{nEdges} \left(\phi_e u_e \frac{\partial u_e}{\partial \mathrm{t}} + \frac{u_e^2}{4} \sum_{i\in CE(e)} \frac{\partial \phi_i}{\partial \mathrm{t}}\right) A_e$$

According to Eq. (63) and (A.8) in Ringler et al. (2010),

$$\left(U,\frac{\partial U}{\partial t}\right)_e = \sum_{e=1}^{nEdges} \phi_e u_e \frac{\partial u_e}{\partial \mathrm{t}} A_e + \sum_{i=1}^{nCells} K_i \frac{\partial \phi_i}{\partial \mathrm{t}} A_i$$

Substituting (4) into above formula

$$\left(U,\frac{\partial U}{\partial t}\right)_e = \sum_{e=1}^{nEdges} \phi_e u_e A_e \left(Q_e^{\perp} + \frac{1}{d_e} \sum_{i\in CE(e)} n_{e,i} E_i\right) + \sum_{i=1}^{nCells} K_i \frac{\partial \phi_i}{\partial \mathrm{t}} A_i$$

According to section 3.7.2 in Ringler et al. (2010),

$$\sum_{e=1}^{nEdges} \phi_e u_e A_e Q_e^{\perp} = 0$$

Since $A_e = l_e d_e$

$$\left(U,\frac{\partial U}{\partial t}\right)_e = \sum_{e=1}^{nEdges} \phi_e u_e l_e \sum_{i\in CE(e)} n_{e,i} E_i + \sum_{i=1}^{nCells} K_i \frac{\partial \phi_i}{\partial \mathrm{t}} A_i$$

where $E_i = K_i + \phi_i$.

According to (A.4) in Ringler et al. (2010),

$$\left(U,\frac{\partial U}{\partial t}\right)_e = \sum_{i=1}^{nCells} E_i \sum_{e\in EC(i)} n_{e,i} \phi_e u_e l_e + \sum_{i=1}^{nCells} K_i \frac{\partial \phi_i}{\partial t} A_i$$

According to (5),

$$-A_i \frac{\partial \phi_i}{\partial t} = \sum_{e\in EC(i)} n_{e,i} l_e \phi_e u_e$$

Therefore,

$$\left(U,\frac{\partial U}{\partial t}\right)_e = -\sum_{i=1}^{nCells} E_i \frac{\partial \phi_i}{\partial t} A_i + \sum_{i=1}^{nCells} K_i \frac{\partial \phi_i}{\partial t} A_i$$

Consider the inner product on cell

$$\left(\phi,\frac{\partial \phi}{\partial t}\right)_i = \sum_{i=1}^{nCells} \phi_i \frac{\partial \phi_i}{\partial t} A_i$$

Thus,

$$\left(U,\frac{\partial U}{\partial t}\right)_e+\left(\phi,\frac{\partial \phi}{\partial t}\right)_i=-\sum_{i=1}^{nCells}E_i\frac{\partial \phi_i}{\partial t}A_i+\sum_{i=1}^{nCells}K_i\frac{\partial \phi_i}{\partial t}A_i+\sum_{i=1}^{nCells}\phi_i\frac{\partial \phi_i}{\partial t}A_i=0$$

Code availability. Idealized Global Spectral Atmospheric Models (GFDL): https://www.gfdl.noaa.gov/idealized-spectral-models-quickstart/ (last access: 3 May 2019). TMCORE is available at https://github.com/TMCORE-Project/TMCORE (last access: 3 May 2019). The digital object identifier for Idealized Global Spectral Atmospheric Models (GFDL) with standard shallow water test cases is http://doi.org/10.5281/zenodo.3249878. The digital object identifier for TMCORE v1.0 is http://doi.org/10.5281/zenodo.3241647.

Author contributions. Lilong Zhou developed the theory, wrote the initial version of TMCORE, implemented the experiments and wrote the manuscript. Jiming Feng and Lijuan Hua revised the context structure of the manuscript and gave some useful technical advices.

Competing interests. The authors declare that they have no conflict of interest.

Acknowledgements. This work was supported by the National Key R&D Program of China (2016YFA0600403) and the General Project of the National Natural Science Foundation of China (Grant 41875134).

References

Akio Arakawa: Computational Design for Long-Term Numerical Integration of the Equations of Fluid Motion: Two-Dimensional Incompressible Flow. Part I. Journal of Computational Physics, 1, 119-143, 1966.

Akio Arakawa and Vivian R. Lam: Computational Design of the Basic Dynamical Processes of the UCLA General Circulation Model. Methods in Computational Physics, 17, 173–265, 1977.

Chen, C., and Xiao, F.: Shallow water model on cubed-sphere by multi-moment finite volume method, Journal of Computational Physics, 227, 5019-5044, https://doi.org/10.1016/j.jcp.2008.01.033, 2008.

Ji, Z. and Wang, B.: Further Discussion on the Construction and Application of Difference Scheme of Evolution Equations (In Chinese). Scientica Atmospherica Sinica, 15(2), 1-10, 1991.

Li, L., Wang, B., Yuqing, W., and Hui, W.: Improvements in climate simulation with modifications to the Tiedtke convective parameterization in the grid-point atmospheric model of IAP LASG (GAMIL), Advances in Atmospheric Sciences, 24, 323-335, https://doi.org/10.1007/s00376-007-0323-3, 2007.

Li, L., Wang, B., Dong, L., Liu, L., Shen, S., Hu, N., Sun, W., Wang, Y., Huang, W., Shi, X., Pu, Y., and Yang, G.: Evaluation of grid-point atmospheric model of IAP LASG version 2 (GAMIL2), Advances in Atmospheric Sciences, 30, 855-867, https://doi.org/10.1007/s00376-013-2157-5, 2013.

Lin, S.-J.: A "Vertically Lagrangian" Finite-Volume Dynamical Core for Global Models, Monthly Weather Review, 132, 2293-2307, 2004.

N.Swarztrauber, P.: Spectral Transform Methods for Solving the Shallow-Water Equations on the Sphere, Monthly Weather Review, 124, 730-744, 1996.

Putman, W. M., and Lin, S.-J.: Finite-volume transport on various cubed-sphere grids, Journal of Computational Physics, 227, 55-78, https://doi.org/10.1016/j.jcp.2007.07.022, 2007.

Ringler, T. D., Thuburn, J., Klemp, J. B., and Skamarock, W. C.: A unified approach to energy conservation and potential vorticity dynamics for arbitrarily-structured C-grids, Journal of Computational Physics, 229, 3065-3090, https://doi.org/10.1016/j.jcp.2009.12.007, 2010.

Shen T., Tian Y., Chen D., Shen X., Sun X., Liang X., Lu W.: Numerical Weather Prediction (In Chinese), 2nd ed., China Meteorological Press, Beijing, 487 pp., 2015.

Skamarock, W. C., Klemp, J. B., Duda, M. G., Fowler, L. D., Park, S.-H., and Ringler, T. D.: A Multiscale Nonhydrostatic Atmospheric Model Using Centroidal Voronoi Tesselations and C-Grid Staggering, Monthly Weather Review, 140, 3090-3105, https://doi.org/10.1175/mwr-d-11-00215.1, 2012.

Skamarock, W. C., Duda, M. G., Ha, S., & Park, S.-H~~. (2018)~~. Limited-Area Atmospheric Modeling Using an Unstructured Mesh. Monthly Weather Review, 146(10), 3445–3460. https://doi.org/10.1175/mwr-d-18-0155.1, 2018.

Thuburn, J., Ringler, T. D., Skamarock, W. C., and Klemp, J. B.: Numerical representation of geostrophic modes on arbitrarily structured C-grids, Journal of Computational Physics, 228, 8321-8335, https://doi.org/10.1016/j.jcp.2009.08.006, 2009.

~~Shen T., Tian Y., Chen D., Shen X., Sun X., Liang X., Lu W.: Numerical Weather Prediction (In Chinese), 2nd ed., China Meteorological Press, Beijing, 487 pp., 2015.~~

Toy, M. D., and Nair, R. D.: A Potential Enstrophy and Energy Conserving Scheme for the Shallow-Water Equations Extended to Generalized Curvilinear Coordinates, Monthly Weather Review, 145, 751-772, https://doi.org/10.1175/mwr-d-16-0250.1, 2017.

Wang, B.: Design of a new dynamical core for global atmospheric models based on some efficient numerical methods, Science in China Series A, 47, 4, 2004.

Wang, B.: An Explicit Multi-Conservation Finite-Difference Scheme for Shallow-Water Equation, Journal of Computational Mathematics, 26, 404-409, 2008.

~~Ji, Z. and Wang, B.: Further Discussion on the Construction and Application of Difference Scheme of Evolution Equations (In Chinese). Scientica Atmospherica Sinica, 15(2), 1-10, 1991.~~

Wang, B., and Ji, Z.: An Explicit Complete Square Conservative Scheme with ~~Ajustable~~Adjustable Time Intervals, ACTA Meteorologica Sinica, 8, 403-409, 1994a.

Wang, B., and Ji, Z.: The Harmonious Dissipative Operators and the Completely Square Conservative Difference Scheme in an Explicit Way Science in China, 37, 462-471, 1994b.

Wang, B., Ji, Z., and Zeng, Q.: A Class of New Explicit Runge-Kutta Schemes, Progress In Nature Science, 6, 195-205, 1996.

Wang, B., and Ji, Z.: Construction and Numerical Test of the Multi-Conservation Difference Scheme, 48, 1016-1020, 2003.

~~Wang, B.: Design of a new dynamical core for global atmospheric models based on some efficient numerical methods, Science in China Series A, 47, 4, 2004.~~

Wang, B., Ji, Z.: The New Numerical Methods for Atmospheric Science with Applications (In Chinese), 1st ed., Science Press, Beijing, pp. 208 ~~pp.~~, ~~1992~~2006.

~~Wang, B.: An Explicit Multi-Conservation Finite-Difference Scheme for Shallow-Water Equation, Journal of Computational Mathematics, 26, 404-409, 2008.~~

Weller, H., Thuburn, J., and Cotter, C. J.: Computational Modes and Grid Imprinting on Five Quasi-Uniform Spherical C Grids, Monthly Weather Review, 140, 2734-2755, https://doi.org/10.1175/mwr-d-11-00193.1, 2012.

Weller, H.: Controlling the Computational Modes of the Arbitrarily Structured C Grid, Monthly Weather Review, 140, 3220-3234, https://doi.org/10.1175/mwr-d-11-00221.1, 2012.

Williamson, D. L., Drake, J. B., Hack, J. J., Jakob, R., and Swarztrauber, P. N.: A Standard Test Set for Numerical Approximations of the Shallow Water Equations in Spherical Geometry, Journal of Computational Physics, 102, 211-224, 1992.

Wu, Z., and Li, J.: Prediction of the Asian-Australian Monsoon Interannual Variations with the Grid-Point Atmospheric Model of IAP LASG (GAMIL), Advances in Atmospheric Sciences, 25, 387–394, 2008.

Zeng Q., Ji Z.: On The Computational Stability of Evolution Equations (In Chinese). Mathematica Numerica Sinica, 1, 79-86, 1981.

Zeng Q., Zhang X.: Available Energy Conserving Schemes for Spherical Baroclinic Primitive Equations (In Chinese). Scientia Atmospherica Sinica., 11, 113-127, 1987.